

## Thesis, COLLÉGIALITÉ

**Auteur :** Schmitz, Louisa

**Promoteur(s) :** Neirinckx, Virginie

**Faculté :** Faculté de Médecine

**Diplôme :** Master en sciences biomédicales, à finalité approfondie

**Année académique :** 2021-2022

**URI/URL :** <http://hdl.handle.net/2268.2/14857>

---

### Avertissement à l'attention des usagers :

*Tous les documents placés en accès ouvert sur le site le site MatheO sont protégés par le droit d'auteur. Conformément aux principes énoncés par la "Budapest Open Access Initiative"(BOAI, 2002), l'utilisateur du site peut lire, télécharger, copier, transmettre, imprimer, chercher ou faire un lien vers le texte intégral de ces documents, les disséquer pour les indexer, s'en servir de données pour un logiciel, ou s'en servir à toute autre fin légale (ou prévue par la réglementation relative au droit d'auteur). Toute utilisation du document à des fins commerciales est strictement interdite.*

*Par ailleurs, l'utilisateur s'engage à respecter les droits moraux de l'auteur, principalement le droit à l'intégrité de l'oeuvre et le droit de paternité et ce dans toute utilisation que l'utilisateur entreprend. Ainsi, à titre d'exemple, lorsqu'il reproduira un document par extrait ou dans son intégralité, l'utilisateur citera de manière complète les sources telles que mentionnées ci-dessus. Toute utilisation non explicitement autorisée ci-avant (telle que par exemple, la modification du document ou son résumé) nécessite l'autorisation préalable et expresse des auteurs ou de leurs ayants droit.*

---

# Study of PTPRZ1 for the specific targeting of pediatric and adult gliomas

**Louisa SCHMITZ**

Master's thesis presented to obtain the degree of  
Master in Biomedical Sciences

Promotor: NEIRINCKX Virginie

Co-promotor: ROGISTER Bernard

Laboratory of Nervous System Disorders and Therapy Giga Neurosciences

Academic year: 2021 - 2022

## Acknowledgements

---

As a preamble to this master's thesis, I would like to gratefully thank the people who helped and supported me throughout this work.

I would like to thank Professor Bernard Rogister, my co-promotor, for inviting me in his laboratory to perform my thesis.

I also sincerely thank my promotor Virginie Neirinckx, who suggested me this interesting subject, and who supervised me throughout this thesis. Thank you for your advice and your consideration, as well as for your support in my work.

I would like to thank all the Bernard Rogister's team for their help in the elaboration of my research included in my thesis and for all the practical pieces of advice, and in particular Marc-Antoine Da-Veiga, who supervised my work and taught me a lot.

I would like to give a special thanks to Gauthier for his unfailing support during those past few years.

Naturally, I also thank my parents for their support and patience during my studies.

Finally, I want to thank my friends for the incredible adventure these past five years has been, including all the good memories and the time spent together.

## Abstract

---

Malignant gliomas, including glioblastoma, are aggressive glial cancers of the central nervous system. Gliomas are classified by grade from 1 to 4 depending on their anatomo-histological characteristic and molecular features. Both in adults and children, gliomas can be classified as “low-grade” or “high-grade”, according to their malignancy, prognosis, and recurrence rate. Therapies include surgery, radiotherapy, and chemotherapy. However, resistance to therapies and recurrence decrease the survival rate. Many therapeutic approaches are in development, such as immunotherapy or targeted therapies, giving hope to gliomas patients.

Protein tyrosine phosphatase receptor type Zeta1 (PTPRZ1) is described in the literature as overexpressed in gliomas. The receptor is also described as present on glioma stem-like cells. Moreover, the receptor could play a role in the tumor cell migration with the help of one of its ligands, the pleiotrophin. Migration of tumor cells in the subventricular zone could be essential in the recurrence of tumors. The research hypothesis for this thesis is that this receptor could be a potential target for adult and pediatric gliomas therapies.

The objective of this thesis is to validate the presence of PTPRZ1 on adult and pediatric cell cultures, as well as to understand the function of the receptor *in vitro*.

To confirm this hypothesis, characterization of the different cell lines as been done with immunofluorescence, qPCR, western blot, viability, and migration assays. These experiments demonstrated the presence of PTPRZ1 in the different cell cultures.

The use of a small inhibitor molecule (NAZ2329) of the receptor allowed to assess the effect of the receptor on cell proliferation. The impact of NAZ2329 and pleiotrophin on migration was also tested but no effect was observed.

## Résumé

---

Les gliomes malins, comme le glioblastome, font partie des cancers les plus agressifs du système nerveux central. Les gliomes sont classés par grade de 1 à 4 selon leurs caractéristiques anatomo-histologiques ainsi que leurs caractéristiques moléculaires. Autant chez l'adulte que chez l'enfant, les gliomes sont dits de « bas-grade » ou de « haut-grade » en fonction de leur agressivité, du pronostic ainsi que des chances de récurrence. Parmi les thérapies existantes, on retrouve la chirurgie, la radiothérapie ainsi que la chimiothérapie. Cependant, la résistance à ces thérapies de même que les récurrences empêchent l'amélioration du taux de survie. En revanche, de nombreuses nouvelles thérapies comme l'immunothérapie et les thérapies ciblées constituent un réel espoir pour les patients atteints de gliomes.

Le sujet de ce mémoire porte sur le récepteur tyrosine phosphatase Zeta1 (PTPRZ1) qui est décrit dans la littérature comme étant nettement surexprimé dans les gliomes. PTPRZ1 est décrit comme présent sur les cellules de gliomes à caractère souche. De plus, ce récepteur jouerait un rôle dans la migration des cellules tumorales grâce à un de ses ligands, la pléiotrophine. La migration de ces cellules dans la zone sous-ventriculaire aurait une grande importance dans la récurrence des gliomes adultes et pédiatriques. L'hypothèse de recherche développée dans ce mémoire est que ce récepteur pourrait être une cible potentielle pour la thérapie de ces tumeurs.

Ainsi, l'objectif de ce mémoire est de confirmer la présence du récepteur PTPRZ1 sur des cellules de lignées adultes et pédiatriques de gliomes mais également d'élucider la fonction que joue ce récepteur *in vitro*.

Pour confirmer cette hypothèse, la caractérisation des lignées cellulaires par différentes analyses comme l'immunofluorescence, la qPCR, le western blot, un test de viabilité ainsi qu'un test de migration ont été réalisés. Ces analyses ont démontré la présence du récepteur dans les différentes lignées de gliomes.

L'utilisation d'une molécule inhibitrice (NAZ2329) du récepteur PTPRZ1 a permis d'observer l'effet qu'induit l'inhibition de ce récepteur sur la prolifération cellulaire. L'effet de NAZ2329 ainsi que la pléiotrophine sur la migration a été également étudié mais aucun effet significatif n'a été observé.

## Abbreviations List

---

- PTPRZ1 = Protein tyrosine phosphatase receptor zeta 1
- OPC = Oligodendrocyte Precursor Cell
- CNS = Central Nervous System
- WHO = World Health Organization
- IDH = Isocitrate Dehydrogenase
- G-CIMP = Gliomas CpG Island Methylator Phenotype
- ATRX = Alpha Thalassemia/mental Retardation Syndrome X-linked
- ALT = Alternative Lengthening of Telomere
- TERT = Telomerase Reverse Transcriptase
- CDKN2A/B = Cyclin-depedent kinase inhibitor 2A/B
- EGFR = Epidermal Growth Factor Receptor
- pLGG = Pediatric Low-grade gliomas
- pHGG = Pediatric High-grade gliomas
- GBM = Glioblastoma
- DIPG = Diffuse Intrinsic Pontine Gliomas
- AA = Anaplastic Astrocytoma
- NF1 = Neurofibromatosis type 1
- GTR = Gross Tumoral Resection
- AYA = Adolescent and Young Adults
- RT = Radiotherapy
- GSC = Glioma Stem Cell
- CSC = Cancer Stem Cell
- SVZ = Subventricular Zone
- SGZ = Subgranular Zone
- LV = Lateral Ventricle
- NPC = Neural precursor cell
- PTN = Pleiotrophin
- TAMs = Tumors-Associated Macrophages

## Table of contents

---

1	Introduction .....	1
1.1	Adult diffuse gliomas .....	1
1.1.1	Epidemiology .....	1
1.1.2	General classification of gliomas in adulthood .....	2
1.1.2.1	Anatomo-pathological features and clinical grading of gliomas .....	2
1.1.2.2	Implementation of molecular features in adult glioma classification .....	3
1.1.2.3	Most important molecular features in adult glioma classification .....	3
1.2	Pediatric diffuse gliomas .....	5
1.2.1	Epidemiology .....	5
1.2.2	General classification of pediatric diffuse gliomas .....	6
1.2.2.1	Clinical grading of diffuse gliomas in children .....	6
1.2.2.2	Molecular features in pediatric low-grade gliomas .....	7
1.2.2.3	Molecular features in pediatric high-grade gliomas .....	8
1.2.3	Current treatment modalities for pediatric gliomas.....	10
1.2.4	Novel therapeutic perspectives for pediatric high-grade gliomas .....	11
1.2.4.1	Targeting of histone mutations .....	11
1.2.4.2	Immunotherapeutic approaches .....	11
1.3	The concept of glioma stem cells .....	12
1.4	The role of the subventricular zone in glioma recurrence .....	13
1.5	Protein tyrosine phosphatase receptor Zeta 1 (PTPRZ1) .....	15
1.5.1	Overview .....	15
1.5.2	Structure and functions.....	15
1.5.3	Implication of PTPRZ1 in targeted therapy for adult and pediatric gliomas .....	18
2	Plan and Objectives .....	19
3	Materials and methods .....	20
3.1	Human cell lines .....	20
3.2	Cell cultures.....	20
3.3	Neurospheres formation assay .....	21
3.4	Processing of neurospheres sections before immunostaining .....	21
3.5	Immunofluorescence .....	21
3.5.1	Cells on coverslips .....	21
3.5.2	Neurospheres .....	22

3.5.3	Adult GBM biopsies.....	22
3.6	Quantitative RT-PCR .....	24
3.7	Western Blot .....	24
3.8	Cell Viability Assay.....	25
3.9	Migration Assay .....	25
3.10	Statistical analysis.....	26
4	Results .....	27
4.1	Expression of PTPRZ1 in glioma cell lines.....	27
4.2	Expression of different isoforms of PTPRZ1 .....	31
4.3	Expression of PTPRZ1 in adult GBM tissue.....	32
4.4	Effect of NAZ2329 on PTPRZ1 function.....	34
5	Discussion .....	38
6	Bibliography.....	44



---

# INTRODUCTION

---

# 1 Introduction

Gliomas are malignant tumors from the central nervous system<sup>1</sup>. These tumors are the most common type of primary brain tumors in adults<sup>1</sup> and children<sup>2</sup>. Gliomas can be separated into two main groups: (1) the circumscribed gliomas and (2) the diffuse gliomas<sup>3</sup>.

Gliomas are presumably arising from glial cells, but the cell of origin is still unknown. However, experimental *in vivo* data demonstrates that many cell types of the brain could be the original cell type of gliomas. Putative target cells involve oligodendrocyte precursor cells (OPCs), astrocytes and neural stem cells<sup>4</sup>.

## 1.1 Adult diffuse gliomas

### 1.1.1 Epidemiology

The malignant brain tumors account for 29.1%, while the non-malignant ones account for 70.9%. Among the non-malignant brain tumors, the most prevalent is meningioma, accounting for 54.5%. Among all malignant CNS tumors, glioblastoma accounts for 49.1% and is the most common<sup>5</sup>. Among gliomas, glioblastoma accounts for the major part with 58.4%<sup>5</sup>.

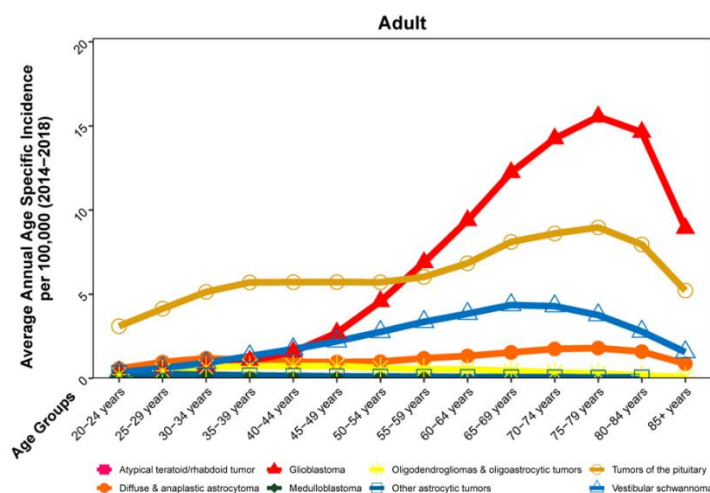


**Figure 1: Incidence by age of brain and other CNS tumors.** The graph shows the average annual age specific incidence from the age of 20 years to 85+ years. Glioblastoma has the most important average annual age specific incidence from 55-59 years to 85+ years (From Ostrom et al., 2021<sup>5</sup>).

The average annual age specific incidence is the most significant for glioblastoma in the age range 55-59 years to 85+ years (**Figure 1**)<sup>5</sup>.

Malignant brain tumors and other CNS tumors are the 26<sup>th</sup> most common cause of death for the people in the age range of 40 years and more<sup>5</sup>.

## 1.1.2 General classification of gliomas in adulthood

Please note that all the classification and epidemiology data were reported before the recent WHO CNS5 report.

### 1.1.2.1 Anatomic-pathological features and clinical grading of gliomas

During the past decades, the classification was built on microscopy characteristics. For the glioma classification, there are different grades characterizing different histological degrees of malignancy and biological behavior of the tumor. The diffuse gliomas include astrocytomas, oligodendrogliomas tumors and oligoastrocytomas. A common feature of these tumors is the widespread infiltration of cancer cells that invade the parenchyma and trap the non-neoplastic cells (**Figure 2A**)<sup>6</sup>.

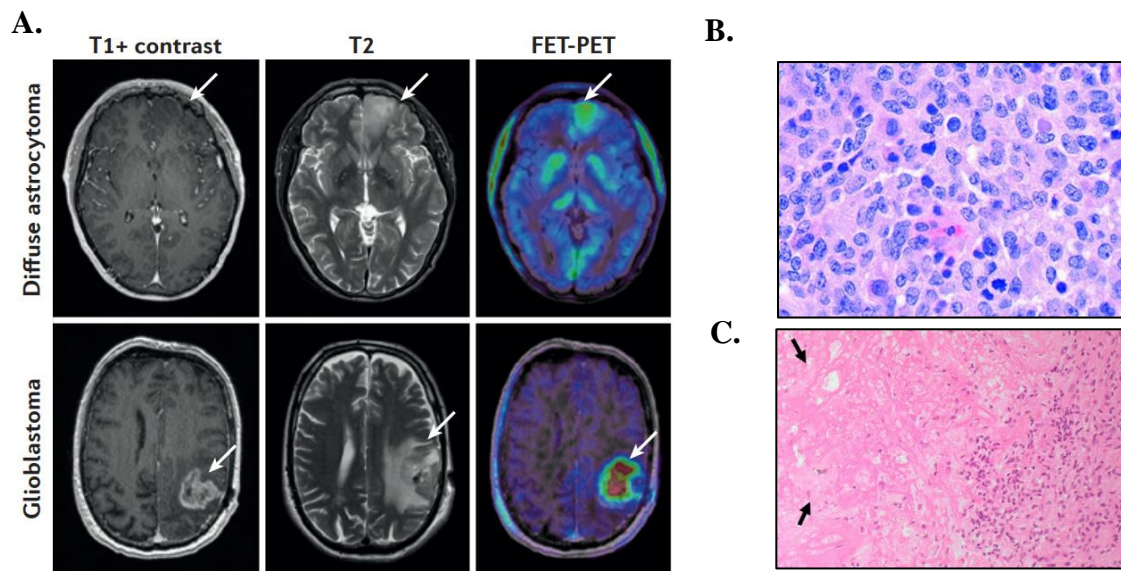


**Figure 2: Neuroimaging and histopathologic features of Diffuse astrocytoma and Glioblastoma.** (A) T1 and T2 are MRI and FET-PET (18F-fluoro-ethyl-tyrosine (FET) amino acid PET) (left to right). (B) Hematoxylin-Eosin staining of astrocytoma. (C) Hematoxylin-Eosin staining showing necrosis (arrows) in glioblastoma (Adapted from Weller et al, 2015<sup>3</sup>, Gupta et al, 2005<sup>6</sup>, Bradshaw et al, 2016<sup>7</sup>).

The oligodendrogliomas usually present round and regular nuclei as well as perinuclear clearing<sup>6</sup>. The oligodendrogliomas are divided in two grades: the oligodendrogliomas, which are grade 2, and anaplastic oligodendrogliomas, grade 3. The grading depends on different features such as necrosis, mitotic activity, cytologic atypia<sup>6</sup>. The first grade indicates a tumor with a low proliferative rate and a potential complete resection<sup>8</sup>.

The astrocytic tumors include the diffuse astrocytomas (grade 2) and anaplastic astrocytomas (grade 3). These are for the most part infiltrative and often recur<sup>8</sup>. The conventional features of astrocytomas are hyperchromatic, irregular nuclei and limited cytoplasm (**Figure 2B**)<sup>6</sup>.

Finally, the most malignant is the glioblastoma (GBM), classified grade 4<sup>8</sup>. GBM is characterized by mitotic activity, necrosis, hypercellularity and invasiveness, which are signs of malignancies (**Figure 2C**)<sup>9</sup>.

### ***1.1.2.2 Implementation of molecular features in adult glioma classification***

As mentioned before, during several years, classification was based on histological criteria. In 2016, it was decided that molecular features needed to be incorporated to the classification. This new classification with molecular features was needed to allow a better management of the patients after the diagnosis<sup>10</sup>. Since then, the histological assessment of the tumors is integrated with the genetic features for tumor grading<sup>10</sup>. In 2021, the WHO published a new classification in which the molecular features, the taxonomy and other changes are updated<sup>11</sup>, indicative of the very fast evolution in the understanding of glioma biology.

### ***1.1.2.3 Most important molecular features in adult glioma classification***

In each subgroup of diffuse gliomas, several mutations orientate the classification (**Figure 3**).

- **IDH mutations:** The isocitrate dehydrogenase 1 or 2 mutations (IDH1/IDH2) affect the amino acid 132 or 172 in the sequence, respectively. In both mutations, an arginine residue is replaced by another, like histidine (i.e. IDH1 mutation R132H)<sup>12</sup>. The isocitrate dehydrogenase enzyme catalyzes the oxidative decarboxylation of  $\alpha$ -ketoglutarate, which produces NADPH in physiological condition. The mutant IDH enzyme produces R(-)-2-hydroxyglutarate. The gain of R(-)-2-hydroxyglutarate and the reduction of NADPH could impact the cells with oxidative stress<sup>3</sup>.

Moreover, the increase level of R(-)-2-hydroxyglutarate results in G-CIMP (Gliomas-CpG island methylator phenotype)<sup>13</sup>, which is hypermethylation of the CpG islands<sup>1</sup>. The IDH1/IDH2 mutations are detected in high frequency in diffuse astrocytomas, oligoastrocytomas and oligodendrogliomas<sup>12</sup>.

- **ATRX loss:** The alpha thalassemia/mental retardation syndrome X-linked (ATRX) gene mutation results in downregulation of the protein expression<sup>14</sup>. The ATRX gene plays a role in the telomere maintenance. This protein has a role in the ALT system, which is the Alternative Lengthening of Telomere system. The ALT system is overexpressed

with the mutation of ATRX. This ATRX mutation is associated to diffuse astrocytomas<sup>15</sup>.

- **1 p/19q co-deletion:** The 1p/19q co-deletion is the result of a deletion of the short arm of chromosome 1 and the long arm of chromosome 19. This co-deletion is present in almost 80% of oligodendrogliomas. The co-deletion is linked with IDH1/2 mutations<sup>16</sup>. This co-deletion is mentioned as a predictive biomarker<sup>3</sup>.
- **TERT mutation:** TERT is the “telomerase reverse transcriptase”. This gene is involved in the telomere maintenance. This molecular feature is associated with oligodendrogliomas. The mutations in the promoter of this gene lead to the expansion of the telomerase activity<sup>15</sup>. The TERT mutation is also associated with the presence of the IDH1 status and 1p-19q co-deletion<sup>17</sup>.
- **Cyclin-dependent kinase inhibitors 2A/B (CDKN2A/B):** Homozygous deletion of CDKN2A/B on 9p21. CDKN2A encodes for p16<sup>INK4A</sup> cyclin-dependent kinase inhibitor, while CDKN2B encodes for p15<sup>INK4B</sup> cyclin-dependent kinase inhibitor<sup>1</sup>. These homozygous deletions provoke dysregulation in signaling pathways implicated in cell cycle<sup>18</sup>. It is a molecular marker of WHO grade 4 IDH-mutant astrocytoma<sup>18,19</sup>.
- **Epidermal growth factor receptor (EGFR):** Amplification of EGFR gene occurs in 50% of glioblastomas. The variant EGFRvIII is also found when EGFR amplification is present. The variant is constitutively active, promoting tumor growth. This variant induces the constitutive overexpression of common pathways sustaining cell proliferation, invasion, and resistance to induction of apoptosis<sup>20</sup>. EGFR amplification is a molecular marker of glioblastoma IDH-wildtype<sup>19</sup>.
- **Histone mutations:** Mutations have been identified in the gene of histone 3 (H3). Mutations can occur in histone H3.1 (*HIST1H3B/C*) or H3.3 (*H3F3A*). These mutations are H3K27M, which is a substitution of lysine by a methionine, or G34 mutations in H3F3A gene, which consist in missense mutations. The mutations affect epigenetic regulation of gene expression<sup>19</sup>. These mutations have been identified in pediatric diffuse intrinsic pontine glioma (DIPG). The H3.3 mutations mainly occur in pediatric gliomas<sup>18</sup>. The histone mutations will be described more precisely in the pediatric section of this thesis.

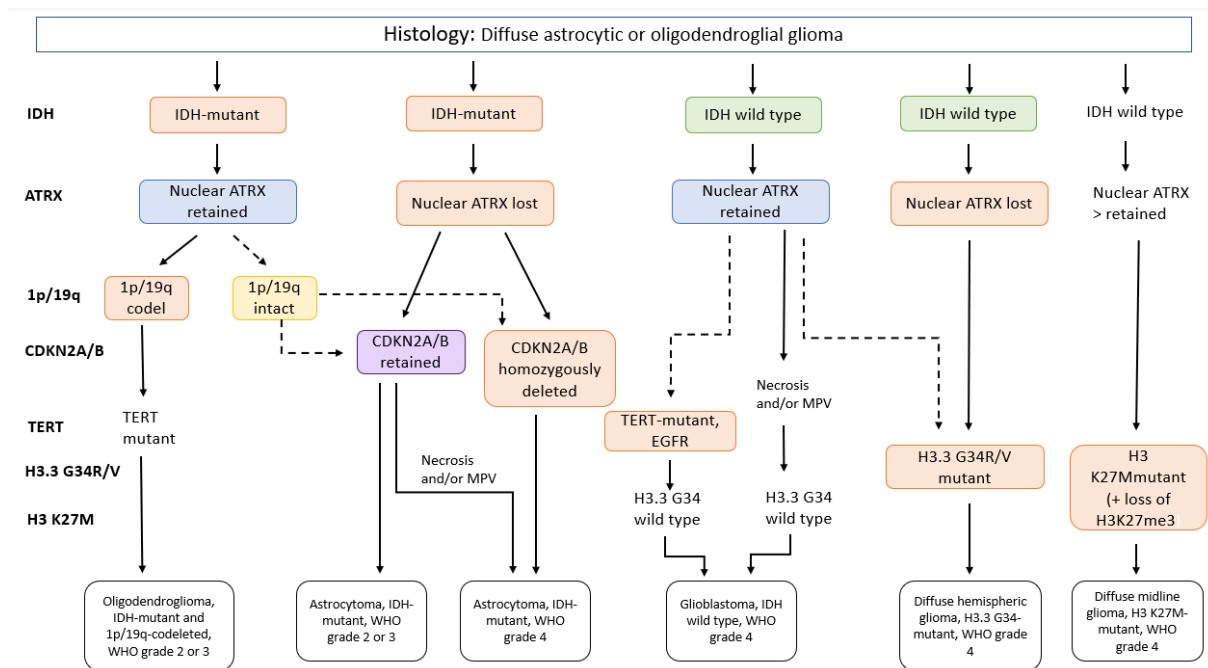


**Figure 3: Adult classification of principal diffuse gliomas depending on most important molecular features.** Main molecular features, which constitute the classification of adult diffuse gliomas from the histology. IDH and ATRX are the first assessed mutations. MPV = microvascular proliferation (Adapted from Weller et al, 2021<sup>19</sup>).

In this thesis, the main focus is on pediatric gliomas. The pediatric classification is based on the same principle than the adult's with histology features, and molecular markers. The pediatric classification of gliomas is described below.

## 1.2 Pediatric diffuse gliomas

### 1.2.1 Epidemiology

According to the CBTRUS report of 2021, primary brain and other CNS tumors are the most common cancer in children (0-14 years) but are in second and eight position for the population between 15-39 years population<sup>5</sup>.

Between 2014 to 2018, for children and adolescent populations (0-19 years), 6% of brain tumors was reported for this age range. In this percentage, gliomas accounted for 45% and represent 18.3% of pilocytic astrocytomas, 5.3% of diffuse and anaplastic astrocytomas and 2.6% of glioblastomas<sup>5</sup>.

The distribution of all primary brain and other CNS tumors in children (0-14 years) slightly change between 2013-2017 and 2014-2018 (**Figure 4**). The brain tumors are the most common cause of cancer death in children (0-14 years), but not in the older populations <sup>5</sup>.

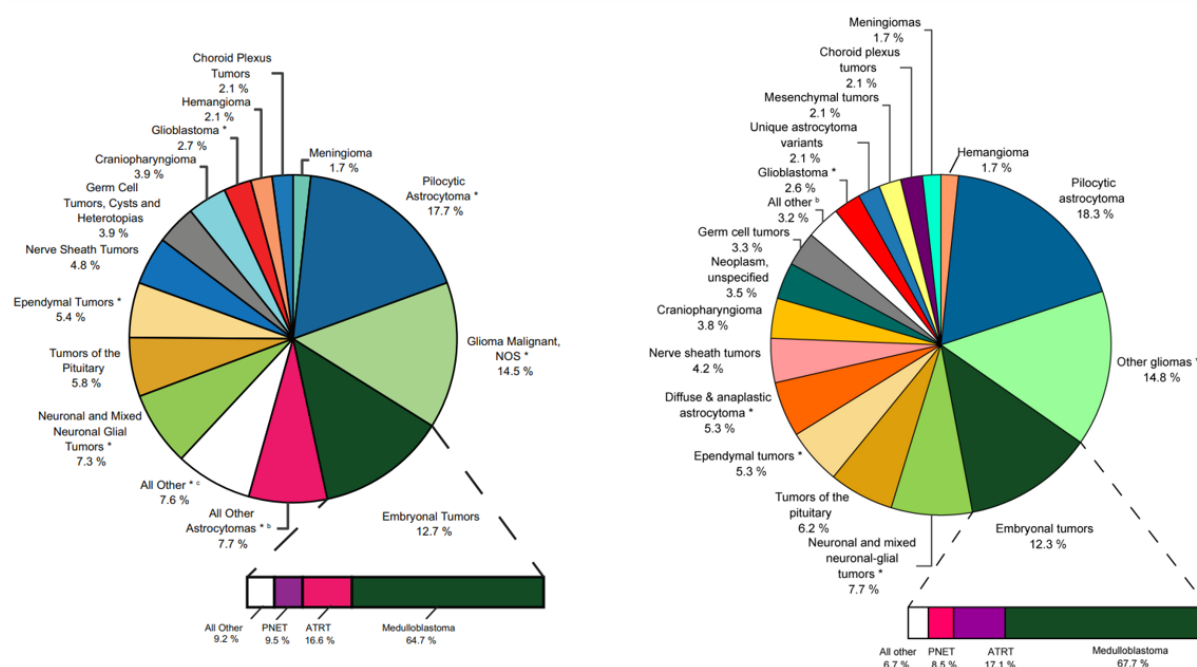


**Figure 4: Distribution in children (0-14 years) of all primary brain and other CNS tumors by histology from CBTRUS 2013-2017 (left) and CBTRUS 2014-2018 (right).** Glioblastoma represents a small percentage 2.7% between 2013-2017 and 2.6% between 2014-2018 (Adapted from Ostrom et al., 2020<sup>21</sup> and Ostrom et al., 2021<sup>5,21</sup>).

## 1.2.2 General classification of pediatric diffuse gliomas

Like in adults, as mentioned before, there are different type of pediatric diffuse gliomas characterized by different histopathology and molecular features. Two main subgroups exist, which are the Low-grade gliomas (LGGs) and the High-grade gliomas (HGGs). Each group contains different subtypes according to their intrinsic characteristics<sup>22</sup>.

### 1.2.2.1 Clinical grading of diffuse gliomas in children

#### Pediatric Low-grade gliomas (pLGGs)

The most common are astrocytomas, which account mostly for pilocytic astrocytoma (WHO grade 1) and diffuse astrocytoma (WHO grade 2), which is more infiltrative<sup>23</sup>. pLGGs are classified as a distinct entity from adult low-grade based on their genetic features<sup>23</sup>.

The genetic alterations found in pediatric gliomas depend on different features, such as the patient's age and the location of the tumor<sup>23</sup>.

#### Pediatric High-grade gliomas (pHGGs)

pHGGs also comprise different subtypes, such as anaplastic astrocytoma (WHO grade 3), diffuse intrinsic pontine glioma (DIPG), and glioblastoma (GBM) (both WHO classified as grade 4)<sup>2</sup>. There are different locations according to the subtypes. The diffuse midline gliomas are found in the thalamus, brainstem, and spinal cord<sup>10</sup>. The others pHGGs are mostly present in hemispheric, supratentorial areas<sup>24</sup>.

With time and continuous investigation, it becomes clear that pediatric and adult gliomas are different entities. Both LGGs and HGGs show different mutations. There are other mutations that seem to be more specific features of childhood gliomas<sup>25</sup>. While the IDH mutations are frequently present in adult gliomas, these mutations are uncommon in children GBM (<10%)<sup>26</sup>.

#### ***1.2.2.2 Molecular features in pediatric low-grade gliomas***

In children, usually, low-grade gliomas do not undergo further malignant transformation<sup>26</sup>.

- **NF1:** A small percentage of children develop LGGs due to a hereditary tumor syndrome called neurofibromatosis type 1 (NF1)<sup>27</sup>. This syndrome is due to constitutional mutation in the tumor suppressor gene neurofibromin 1 (NF1) located on chromosome 17q. With this syndrome, there is a downregulation of the raf and PI3K pathways, resulting in cellular proliferation. Patients with NF1 syndrome need additional genetic features to develop high-grade gliomas<sup>23</sup>.
- **MAPK/ERK deficiencies:** In low-grade gliomas, the oncogenesis accounts with MAPK/ERK deficiencies<sup>27</sup>. BRAF is a protein implicated in the MAPK/ERK pathway<sup>28</sup>. Alterations in BRAF gene commonly occur. The V600E mutation is the replacement of a valine at codon 600 by glutamic acid resulting in the activation of the BRAF domain<sup>23</sup>. Moreover, fusion protein of the BRAF and KIAA1549 genes on chromosome 7q is common<sup>1</sup>, resulting in the constitutive activation of the RAS/MAPK pathway<sup>29</sup>.
- **MYB/MYBL1:** In younger patients with diffuse astrocytoma, the MYB (v-myb avian myeloblastosis viral oncogene homolog) or MYBL1 (v-myb avian myeloblastosis viral oncogene homolog-like 1) rearrangement mutations are preferentially occurring<sup>27</sup>. The MYB and MYBL1 rearrangements are associated with a deletion of the C-terminal



region. The mechanism of MYB oncogenesis is not well established. It is suggested that there is an activation of MAPK pathways<sup>30</sup>.

### ***1.2.2.3 Molecular features in pediatric high-grade gliomas***

- ***Histone H3 mutations:*** Somatic mutations were identified in histone H3 genes<sup>26</sup>. The mutations have been identified more commonly in the H3FA gene (>70%), which are the H3.3 mutations. However, it can also be found in HIST1H2B/C genes (<30%), making the H3.1 mutations<sup>31</sup>. Among these mutations, there is the K27M, which is a substitution of a lysine by a methionine. There is also G34R/V, which is a substitution of a glycine by an arginine or a valine amino acid<sup>32</sup>.

The H3.3-K27M mutation is acting on di- and trimethylation. The reduction of this epigenetic mark is provoked by the inhibition of Polycomb repressive complex 2 (PRC2 complex) by interaction with the enzymatic EZH2 domain<sup>33,34</sup>.

The K27M mutation is found in the diffuse intrinsic pontine gliomas (DIPGs) from the midline glioma subgroup. The G34R/V mutation is found in supratentorial GBM, but not in the DIPG. The two kinds of mutations seem to be correlated with age and location<sup>32</sup>. In an integrative genomic approach, K27 cluster shows to be essentially present in children around ten years old, while the G34 cluster shows presence in adolescent and young adult<sup>26</sup>.

- ***Platelet-derived growth factor receptor alpha (PDGFR $\alpha$ ):*** Platelet-derived growth factor receptor alpha is a receptor that is often mutated in pHGGs. The somatic mutations comprise missense mutations, in-frame insertions, or deletion. Experiments demonstrate that the mutants PDGFR $\alpha$  are constitutively active, which give rise to activation of downstream signaling pathways<sup>35</sup>.

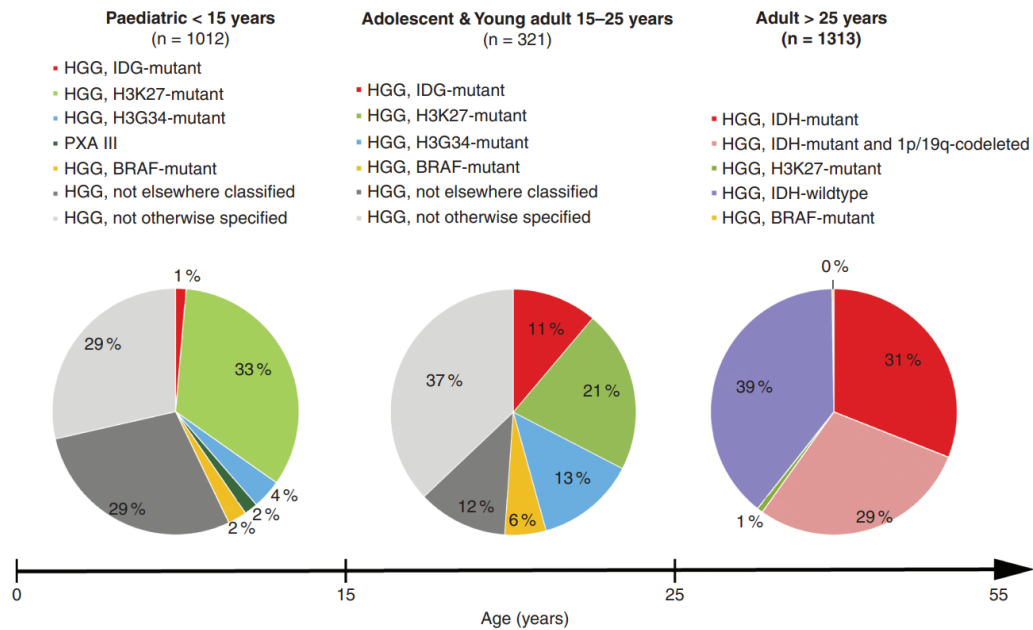


**Figure 5: Comparison of mutations in pie chart in different age groups of HGG.** The graphs show the distribution of mutations in HGG according to age. In pediatric subgroups, the H3K27-mutant is predominant. While in adults, the IDH-mutant is predominant (From Roux et al., 2020 <sup>36</sup>).

The molecular parameters are specific to the patients' age (**Figure 5**) and help to orientate the diagnosis and establish prognostic factors<sup>11</sup>. As the different tumor grades are associated with different gene expressions and these are associated to various survivals, the grade guides the clinical strategies<sup>37</sup>.

Moreover, in children, there are parameters like age (in relationship with molecular parameters) and location of tumor that affect the emergence of the clinical signs and symptoms of the tumors. Among very young children up to 3 years old, the tumor location is mostly supratentorial. The older children between 4 and 10 years old have a tumor location more infratentorial<sup>2</sup>. DIPG located in the pons rapidly presents specific symptoms like cerebrospinal fluid obstruction. The hemispheric tumors more present in adolescent show a small increase of survival<sup>25</sup>.

### 1.2.3 Current treatment modalities for pediatric gliomas

First, the approaches of treatment for the patient are very different depending on the types of gliomas<sup>38</sup>.

For adult treatment modalities, the standard treatment is surgery, radiotherapy, and chemotherapy. For circumscribed gliomas as pilocytic glioma, the surgery can be curative. However, for diffuse gliomas, total resection is hardly possible. The chemoradiotherapy regimen is composed of 30 fractions of 60 Gy with everyday temozolomide<sup>1</sup>.

As mentioned above, there are major molecular differences between the adults and children/adolescent populations. Therefore, the management cannot be the same<sup>39</sup>.

For the pLGGs, the first approach is the surgery when it is possible<sup>38</sup>. The gross total resection (GTR) can be curative in pilocytic astrocytomas as it is a circumscribed glioma. The GTR should be tried in all different types of LGGs<sup>40</sup>. Next, the standard therapy is “watch and wait”<sup>38</sup>. In case of additional therapy, the chemotherapies used are Vincristine adding with Carboplatin, or Vinblastine as a monotherapy. As opposed to the results in adult patients, the temozolomide do not seem to provide better outcome than the standard therapy for pediatric LGG<sup>25</sup>.

For pHGGs, maximal resection is employed, when possible, followed by radiotherapy (patients older than 4 years) and chemotherapy<sup>25</sup>. Based on adult positive result data for temozolomide adding to radiotherapy<sup>41</sup>, the temozolomide is considered as therapeutic foundation for these pHGGs<sup>25</sup>. However, pHGGs are very heterogeneous tumors, meaning that a single drug has little possibility to act on a large group of patients<sup>25</sup>. In pediatric and AYA (adolescents and young adults), the radiotherapy is composed of 1.8 Gy size delivering 59.4 Gy in 33 fractions to reduce the late effects of RT<sup>40</sup>.

For the DIPGs, the tumor is in the brainstem and surgery is impossible because of the presence of cranial nerves nuclei<sup>42</sup>. The standard treatment for this kind of tumor is radiotherapy, which improves the quality of life (palliative)<sup>25,39</sup> for a time, but almost never increases survival<sup>25</sup>.

Regardless of the different treatment employed for the management of patients, the survival has not considerably improved during these past decades. New pathogenesis-based therapies are made to target specific features of the gliomas. In these new therapies, there are the target therapies of signaling pathways<sup>1</sup> and immunotherapy<sup>43</sup>.

## **1.2.4 Novel therapeutic perspectives for pediatric high-grade gliomas**

### ***1.2.4.1 Targeting of histone mutations***

Diffuse intrinsic pontine glioma (DIPG) frequently includes histone mutations as the H3.3 K27M mutation. Epigenetic modifying agents like demethylase inhibitors and histone deacetylase inhibitors have been made to target the histone mutations<sup>44</sup>. Demethylase inhibitor GSKJ4 inhibits the K27 demethylase JMJD3. This agent maintains the methylation and demonstrates anti-tumor activity *in vitro* and *in vivo*<sup>45</sup>. Panobinostat is another pharmacological agent, acting as histone deacetylase, enhancing H3 acetylation and moderately acting on hypo-trimethylation as well. These two agents seem to have a synergistic effect<sup>46</sup>.

### ***1.2.4.2 Immunotherapeutic approaches***

As already mentioned, one of the principal difficulties to treat the glioblastoma is the immunosuppressive environment. The glioblastoma is designed as a cold tumor, which increases the rapidity of tumor growth and promotes recurrence<sup>37</sup>.

There are different immunotherapy approaches to tackle glioblastoma: vaccination, immune-checkpoint blockade, CAR-T cell therapy<sup>1</sup> and virotherapy<sup>47</sup>.

The virotherapy allows to recruit immune cells such as cytotoxic T cells, which drive the tumor more “hot tumor” and responsive to the immune system. Three types of viruses have been widely investigated: the herpes simplex virus, the adenovirus and poliovirus<sup>47</sup>.

Oncolytic viruses have different advantages such as the selective replication in cancer cells, lack of resistance, and the capacity to enhance immune response. Two mechanisms can bring antitumor responses for the success of the therapy. The first one is the lysis of the cancer cells while the second mechanism is a raise of immune response against the tumor cells induced by the release of neoantigens in the microenvironment. The future perspective for this therapy is the combination with other therapeutics approaches<sup>48</sup>.

Another therapeutic approach is the CAR-T cell therapy. CAR, which means “chimeric antigen receptor”, is an engineered receptor with an extracellular antigen-recognition domain that can recognize a specific antigen<sup>49,50</sup>.

CAR-T cells are composed of three different parts: the ectodomain, which is the signal peptide formed by the variable portion of heavy and light chains of an immunoglobulin, the transmembrane domain and the endodomain, which contains the CD3 $\zeta$  domain<sup>50</sup>. The

intracellular domain of third generation, which are named as the signaling domain, is composed of CD3 $\zeta$  domain and two co-stimulatory domains. These costimulatory domains are usually CD28, OX40 or 4-1BB<sup>49</sup>.

A study realized on patient-derived H3K27M mutant diffuse midline glioma cells demonstrated the high expression of disialoganglioside GD2 protein. An engineered anti-GD2 CAR T-cells with 4-1BB costimulatory domain demonstrated strong antigen-dependent cytokine generation and the death of diffuse midline gliomas cells *in vitro*<sup>51</sup>. Recently, phase I clinical study with four patients treated with GD2-CAR T cells demonstrated improvement, which makes this therapeutic approach promising<sup>52</sup>.

### 1.3 The concept of glioma stem cells

For several years, studies demonstrate that glioma stem cells (GSCs) could be the source of the recurrence and the resistance to treatment<sup>43</sup>. Malignant gliomas are known to be resistant to therapies, which could explain the poor prognosis of the patients. This tumor resistance could be due to the presence of stem-like cells<sup>53</sup>.

In adult brain tumors, the identification of cancer stem cells (CSCs) has first been suggested by the detection of CD133 (prominin-1) positive cells<sup>54</sup>. *In vitro*, these cells can form spheres from a single cell. It proves the self-renewal capacity of these cancer stem cells<sup>54</sup>. These cells also have the capacity to differentiate and recapitulate the initial phenotype of the primary brain tumor<sup>54</sup>.

Another evidence of the self-renewal of these CD133+ cancer cells is the ability to perform serial transplantation from a mouse to another and the important fact that the phenotype of the tumor recapitulates the primary tumor of patient<sup>55</sup>. More recently, these CD133+ cells appear to employ different cells division methods. With the use of lineage tracing analysis, it appears that these cells seem to use the symmetric divisions with expanding or differentiating divisions and asymmetric divisions<sup>53</sup>. The division mode appears to rely on the presence of growth factors. Effectively, without growth factors, the symmetric division decreases<sup>53</sup>.

Therefore, different criteria have been established to characterize the GSCs. These functional characteristics are self-renewal, persistent proliferation, tumor initiation, frequency in the tumor, stem cell markers and ability to differentiate along multiple lineages (**Figure 6**)<sup>56</sup>.

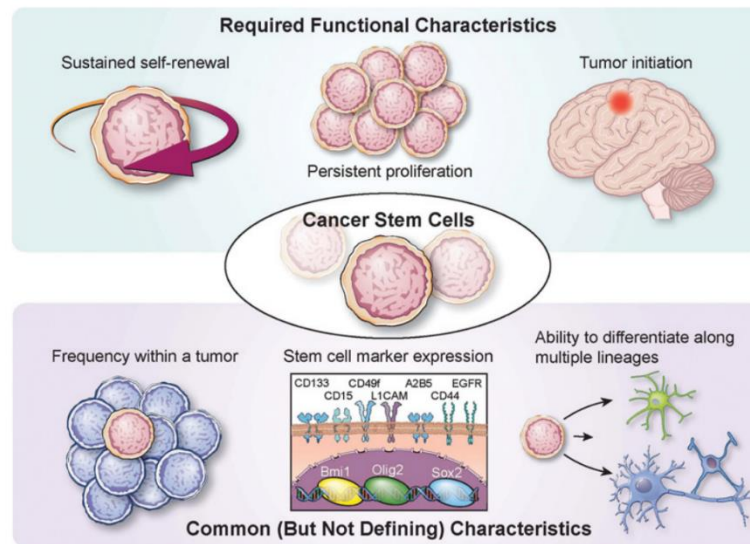


**Figure 6: Functional characteristics of adult GSCs.** Different criteria have been established to define the GSCs such as self-renewing, persistent proliferation, tumor initiation, frequency, putative stem cell markers and ability to differentiation in different lineages. (From Lathia et al, 2015<sup>56</sup>)

Different putative stem cells markers have been reported in pHGGs such as (non-exhaustive list) CD133 (prominin-1), L1CAM (L1 Cell Adhesion Molecule), Nestin which is a neuroepithelial stem cell protein, Sox2 (Sex-determining region Y (SRY)-box2) a transcription factor, CD44 or CD15<sup>24</sup>.

#### 1.4 The role of the subventricular zone in glioma recurrence

In the adult human brain, there are two known neurogenic zones, which are the subventricular zone (SVZ) and the subgranular zone (SGZ) of the *dentate gyrus*, located near the lateral ventricle (LV) and in the hippocampus, respectively. The SVZ is composed of 4 different layers of cells classified from the innermost to the outermost layer<sup>57</sup>.

Some studies revealed that patients with glioblastoma bordering the lateral ventricle and the subventricular zone were associated with decreased survival<sup>58,59</sup>. In the SVZ, a population of GSCs (described above) is found. These GSCs seemed to leave the tumor mass to reach the SVZ via the *corpus callosum*<sup>57</sup>. In fact, a study showed that human GBM cells injected into the striatum of mice demonstrates a tendency to invade the SVZ. As these GSCs can invade the SVZ, this neurogenic zone could be a nest for these cancer-initiating cells<sup>60</sup>.

It has been proven that the SVZ secretes a chemoattractant, CXCL12. The binding of this ligand to its receptor CXCR4 attracts the GSCs to the SVZ<sup>61</sup>. Moreover, CXCL12 appears to mediate GBM resistance to radiotherapy. Indeed, GSCs have revealed to assess mesenchymal features upregulated by CXCL12<sup>62</sup>. A retrospective study demonstrates that pediatric high-grade gliomas, in close contact with the SVZ, were also correlated to a decrease survival as the adult population<sup>63</sup>.

This information leads to the second signaling axis underlying GSC migration to the SVZ. Qin et al demonstrated indeed that pleiotrophin (PTN), which is described as a chemoattractant secreted by the neural precursor cells (NPCs), causes the migration of GSCs to the SVZ. Their study demonstrated that PTN, HSP90B and SPARC/SPARCL1 form a chemoattractant complex. Therefore, the complex allows the activation of Rho/ROCK pathway which acts on the migration of glioma cell (**Figure 7**)<sup>64</sup>. Qin et al. demonstrated this SVZ invasion with DIPG cell lines. One of the receptors of the pleiotrophin is the protein tyrosine phosphatase receptor type  $\zeta$  (PTPRZ1)<sup>64</sup>.

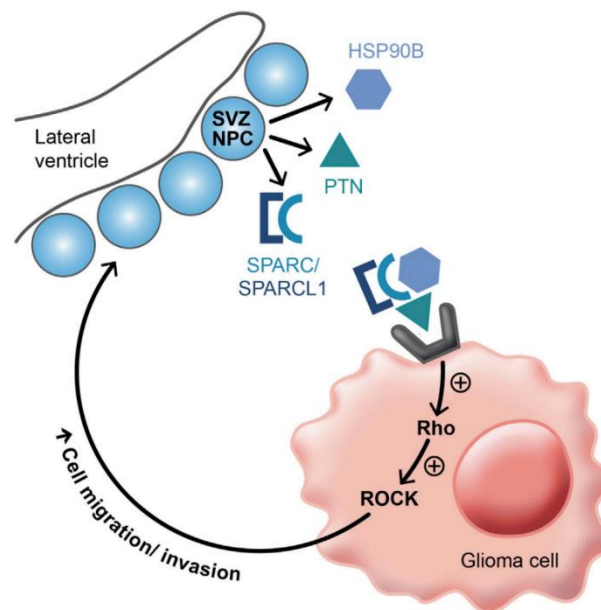


**Figure 7: Representation of glioma cell migration/invasion in the SVZ.** A chemoattractant complex formed by the pleiotrophin (PTN), HSP90B, SPARC/SPARCL1 secreted by the neural precursor cells activate the Rho/ROCK pathway which plays a role in the cell migration (From Qin et al, 2017<sup>64</sup>).

## 1.5 Protein tyrosine phosphatase receptor Zeta 1 (PTPRZ1)

### 1.5.1 Overview

The protein phosphatases have a critical role in the regulation of oncogenic pathways in GBM cells. Three types of classical phosphatases coexist. The protein serine/threonine phosphatases (PSPs), the protein tyrosine phosphatases (PTPs) and the dual specificity phosphatases (DUSPs). The protein phosphatases are able to act like negative oncogenic regulators by dephosphorylating some signaling substrates. PTPRZ1 belongs to the protein tyrosine phosphatases group<sup>65</sup>.

### 1.5.2 Structure and functions

The receptor protein phosphatase type zeta 1 (PTPRZ1) is a member of the R5 subfamily of protein tyrosine phosphatases<sup>66</sup>. The PTPRZ1 protein (**Figure 8**) is composed of a carbonic anhydrase (CAH)-like domain, fibronectin type III-like domain and a large cysteine-free, serine glycine-rich region in its extracellular fragment as well as two tyrosine phosphatase domains (D1 and D2) in its intracellular fragment<sup>66–68</sup>. The two intracellular domains are proximal D1 and distal D2. The D1 domain is active while D2 is inactive<sup>69</sup>.

Different variants are generated by alternative splicing. The PTPRZ-A which is the longest variant, PTPRZ-B which is the short form of the receptor because it lacks an extracellular portion<sup>70</sup>, and finally the PTPRZ-S which is the soluble form also called phosphacan, is the extracellular form that is secreted (**Figure 8**)<sup>65,71</sup>.

The two transmembrane variants are expressed mostly in glial precursors cells while the soluble form, the phosphacan, is mainly expressed in mature glia in the adult brain<sup>65,72</sup>.



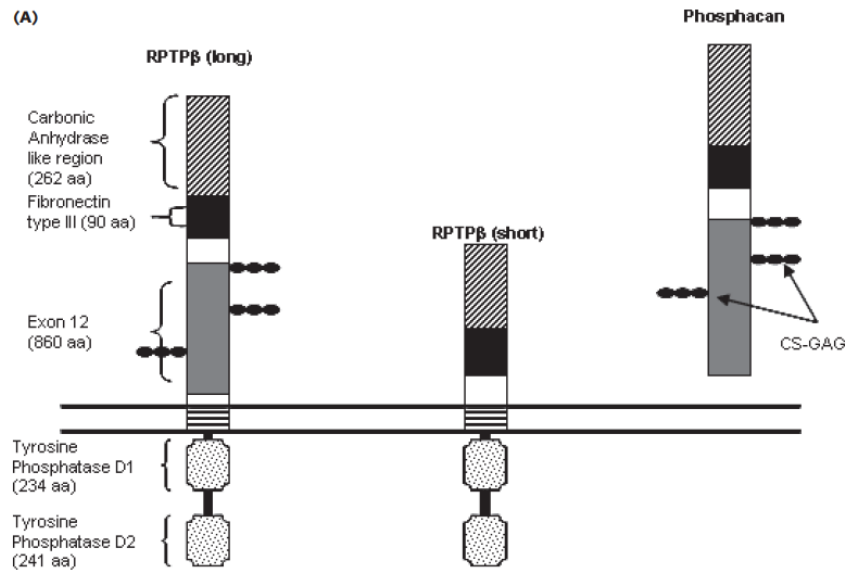


**Figure 8: Representation of three isoforms of PTPRZ1 (PTPRZ1-A= long form, PTPRZ1-B= short form, Phosphacan= soluble form) (From Lorente et al, 2005<sup>73</sup>).**

Research in adult mice's brains demonstrated that the receptor can be cleaved in the extracellular region by metalloproteinases. In contrast, the membrane-tethered fragment is cleaved by presenilin- $\gamma$  secretase, which released the intracellular domain in the cytoplasm. The intracellular domain has been found at nuclear localization. Besides the PTPRZ-S, the soluble form also called phosphacan, soluble forms of PTPRZ-A and PTPRZ-B have also been found in adult mouse brain<sup>74</sup>.

Different soluble ligands can bind to the extracellular portion of the receptor such as pleiotrophin (PTN), midkine (MK), interleukine-34 (IL-34). The interaction between these ligands and PTPRZ1 induces the phosphorylation of different substrates which enhances activation of different pathways<sup>75</sup>. The pleiotrophin (PTN) and midkine (MK) belong to the heparin binding growth factors family. PTN is described as highly preserved among different species. This neurite outgrowth factor seems to be important for migration and angiogenesis<sup>75</sup>.

The PTN binds to the extracellular portion of the receptor. This binding inactivates the receptor phosphatase activity, which leads to an improved tyrosine phosphorylation status of downstream molecules implicated in various signaling pathways like b-catenin (**Figure 9, right**)<sup>76</sup>.

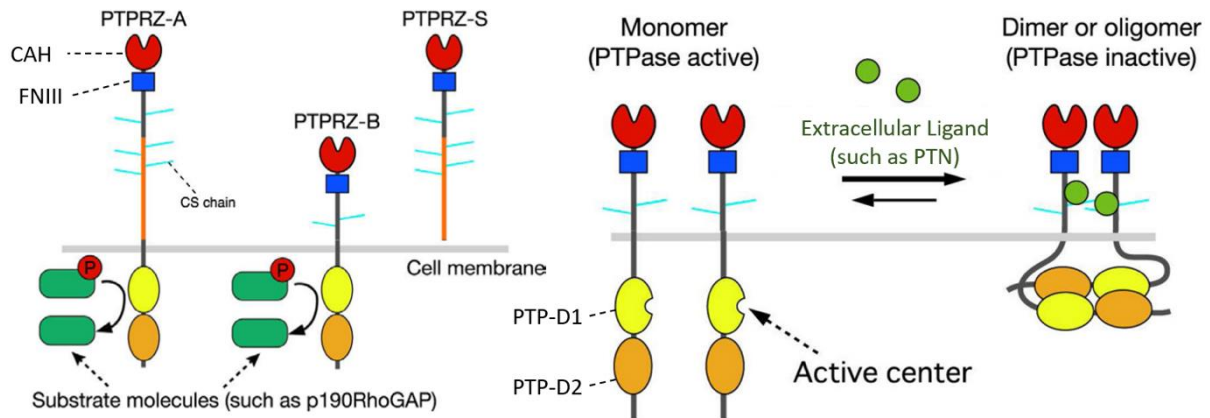


**Figure 9: Representation of Protein tyrosine phosphatase receptor-type Z (PTPRZ) and its activation/inactivation.** PTPRZ1 comprises 3 isoforms containing CAH (carbonic-anhydrase-like domain), FNIII (fibronectin type III domain), CS chain (chondroitin sulfate), PTP-D1 (proximal domain), PTP-D2 (distal domain) (**Left panel**). Representation of the neutralization of the negatively charged CS chain by positively charged ligand PTN (**Right panel**) (Adapted from Fujikawa and Noda, 2016<sup>77</sup>).

The PTPRZ1 proteins are able to dephosphorylate different substrate molecules (**Figure 9, left**)<sup>77</sup>. Some research studies indicate that the chondroitin sulfate chains are charged negatively, which produces a repulsion between receptors. Ligand such as PTN is positively charged. The PTN induces PTPRZ1 clustering by neutralizing the negatively charged chondroitin sulfate<sup>68</sup> (**Figure 9, right**). PTPRZ1 presents a canonical-PDZ binding motif that allows the receptor to interact with different substrates such as PSD-95 (postsynaptic density-95), for example<sup>75</sup>. The physiological importance of the PTPRZ1 gene has been investigated by studying PTPRZ1-deficient mice that presented impairment in hippocampal functions in a maturation-dependent manner<sup>78</sup>. The interaction between PTN and PTPRZ1-A seems to have an impact on the oligodendrocyte differentiation and controlling the timing of differentiation step between oligodendrocyte precursor cells (OPCs) and mature oligodendrocytes<sup>79</sup>.

The different isoforms seem to have different physiological roles. A study shows that overexpressing the short form PTPRZ-B supports dendritic arborization, whereas the overexpression of the long form PTPRZ-A reduces the dendritic arborization but enhances the dendritic growth<sup>80</sup>.

The receptor and one of its ligands (PTN) are overexpressed in human GBM compared to normal brain<sup>81</sup>. Knockdown of PTPRZ1 allowed to determine a functional role of the receptor

in the cell migration. PTPRZ1-B knockdown shows *in vitro* a decrease of migration and proliferation of glioma cells and seems to inhibit tumor growth *in vivo*<sup>82</sup>.

The migration of the cells seems to be affected by a concentration-dependent stimulation of PTN-PTPRZ1 signaling pathway<sup>76</sup>. In contrast, cells without PTPRZ1 did not respond to PTN stimulation<sup>76</sup>. Interestingly, the migration of cells may rely on the extracellular domain whereas the intracellular carboxyl terminal PDZ domain could play a role for the proliferation. The rescued expression of the extracellular domain in GBM cells after the knockdown of PTPRZ1 regenerates the migration but not the proliferation<sup>82</sup>.

Moreover, a study identified the receptor PTPRZ1 as a binding partner of VEGF (vascular endothelial growth factor), which governs angiogenic functions of endothelial cells. The contact of VEGF and PTPRZ1 does not appear to be altered by anti-VEGF drugs. This interaction between the receptor and the VEGF could be a likely explanation of the resistance developed against anti-VEGF therapies<sup>83</sup>. Finally, stable PTPRZ1 knockdown impaired the expression levels of stem cell transcription factors such as Sox2, OLIG2 and POU3F3. PTPRZ1 is observed thus to maintain the stem cell properties in GBM cells. In the same line, this knockdown also reduced the sphere-forming capacity of GBM cells<sup>84</sup>.

### **1.5.3 Implication of PTPRZ1 in targeted therapy for adult and pediatric gliomas**

According to the literature mentioned above, PTPRZ1 seems to be present in different types of gliomas and seems to have an important role in the tumor progression. It provides confidence that PTPRZ1 could be a specific target for CAR-T cells and/or oncolytic viruses. These targeted therapies against PTPRZ1 could indeed focus on the gliomas stem-like cells.

---

# PLAN AND OBJECTIVES

---

## 2 Plan and Objectives

---

A study shows that the secretion of chemoattractive signals by neural precursor cell (NPC) could be implicated in the tendency of gliomas to invade the subventricular zone. With their analysis on diffuse intrinsic pontine gliomas (DIPG), authors demonstrated that the pleiotrophin, which is a neurite outgrowth factor, could be the chemoattractant secreted by the NPC and implicated in the migration of the cancer cells<sup>64</sup>.

Those results lead to suggest that the **receptor protein tyrosine phosphatase type  $\zeta$  (PTPRZ1)**, which is the receptor of the **pleiotrophin**, might be implicated in the proliferation and the migration of the cancer cells and could be thus a **potential target** for the treatment of pediatric and adult gliomas.

During this master's project, we investigate the expression of PTPRZ1 by different cell lines of pediatric and adult gliomas, and the potential difference of expression of PTPRZ1 between the low- and high-grade gliomas. The validation of the expression of the receptor will indeed provide information regarding the relevance to consider this receptor as a potential target.

Moreover, we need to confirm that the receptor has a role in the migration. Migration assays will be performed in presence of pleiotrophin and/or in presence of an inhibitor of the receptor to assess its possible role in the migration of the cancer cells.

Those experiments will strengthen our belief that this receptor could be a potential target for the treatment of pediatric and adult gliomas.

---

# MATERIALS AND METHODS

---

## 3 Materials and methods

### 3.1 Human cell lines

All the experiments have been done on four pediatric cell cultures and one patient-derived adult cell culture (**Table 1**).

<b>Res259</b>	Astrocytoma (pLGG)	Female	4 years old
<b>KNS42</b>	Glioblastoma (pHGG)	Male	16 years old
<b>HSJD-DIPG-007</b>	Diffuse intrinsic pontine glioma	NA	6 years old
<b>HSJD-DIPG-012</b>	Diffuse intrinsic pontine glioma	NA	6 years old
<b>T013</b>	Adult Glioblastoma	NA	42 years old

**Table 1:** Cell cultures used for all the experiments.

Res259, KNS42, DIPG007 and DIPG012 cell lines came from collaborations with Dr Samuel Meignan from Lille. T013 cells were seeded in culture from a human adult GBM tumor resected at the Neurosurgical Department in 2018 (CHU of Liège, Liège, Belgium).

### 3.2 Cell cultures

Human Res259, KNS42 adherent cells were cultivated in DMEM-F12 (Gibco, 31331-028) containing 10% of fetal bovine serum (FBS) (Gibco, 10270-106) and with 1% of streptomycin and penicillin (biowest, MS00WX1007). Human DIPG007, DIPG012 and T013 cells were cultivated in NPC medium containing DMEM-F12 (Gibco, 31331-028), B27 without vitamin A (1/50) (Gibco, 12587-010), 1% of penicillin/streptomycin (biowest, MS00WX1007), 0,2% of normocine (InvivoGen™, ant-nr-2) and heparin (1/25000) (Heparine LEO, 25.000 I.E./U.I/ 5ml).

All cultures in NPC medium were supplemented every second day with 20 ng/ml of human EGF (epidermal growth factor, PeproTech®, AF-100-15-500UG) and 20 ng/ml of human FGF-basic (basic fibroblast growth factor, PeproTech®, 1000-18B-500UG). Human Res259, KNS42 also were cultivated in NPC medium for the neurosphere formation.

### **3.3 Neurospheres formation assay**

All cell types were cultivated into neurospheres in NPC medium (see composition above) in T25 flasks, every second day supplemented with 20 ng/ml of EGF (epidermal growth factor, PeproTech®, AF-100-15-500UG) and 20 ng/ml of FGF2 (basic fibroblast growth factor, PeproTech®, 1000-18B-500UG). The complete medium was changed every two days to allow the growth of the neurospheres.

### **3.4 Processing of neurospheres sections before immunostaining**

The neurospheres were fixed with 4% PFA at RT for 10 minutes, washed thrice in PBS-1x and cryoprotected overnight at 4°C in a solution of sucrose (sucrose 30%, Azide pH 7,4). Neurospheres were frozen in Tissue-Tek OCT in dry ice and preserved at -80°C. The sections were cut at 16 µm thick using a cryostat (NX70).

### **3.5 Immunofluorescence**

#### **3.5.1 Cells on coverslips**

Glass coverslips were coated with Poly-L-ornithine (Sigma, P4638-100MG) 1/10 (Poly-L-Ornithine in H<sub>2</sub>O) for 2 hours. The cells were seeded on each coverslip for 2 days. The cells were fixed with PFA 4% for 15 minutes and washed thrice with PBS-1x. Cells were permeabilized with PBS-T 0.1% (PBS 0.1% tritonX) for 10 minutes. Cells were incubated with TrueBlack 1x in EtOH 70% (Biotium, #23007) for 30 seconds each. Blocking was performed with Normal Donkey serum (Jackson ImmunoResearch, #017-000-121) 10% in PBS-1x for 1 hour. The primary antibodies were incubated overnight at 4°C (see **table 2**). The secondary antibodies were incubated at RT for 1 hour (see **table 3**). The cells were washed thrice with PBS-1x after each step from the primary antibody step. DAPI (1/10000, Sigma-Aldrich®, #D9542) was used to color the nuclei. The DAPI was incubated at RT for 10 minutes. The cells were washed thrice with H<sub>2</sub>O. The coverslips were dried and fixed with safemount QPath® (VWR™ chemicals, #00647520) on slides. Images were taken with an ApoTome Zeiss microscope.



### 3.5.2 Neurospheres

Neurospheres sections were dried at 60°C in oven for 30 minutes. Sections were incubated with consecutive Ethanol solution (EtOH 50%, 70%, 100%) for 5 minutes each. Sections were washed twice with H<sub>2</sub>O for 2 minutes. Antigen retrieval was performed with TRIS-EDTA (pH 9.0, 10 mM Tris base, 1 mM EDTA, 0.05% Tween 20). Blocking was performed with Normal Donkey serum (10% Normal Donkey Serum in PBS-T 0.1% (PBS 0.1% tritonX)) was performed at the same time of permeabilization during 1 hour of incubation. The primary antibodies were incubated overnight at 4°C (see **table 2**). The secondary antibodies were incubated at RT for 1 hour (see **table 3**). The slides were washed thrice with PBS-1x after each step from the primary antibody step. DAPI (1/10000, Sigma-Aldrich®, #D9542) was used to color the nuclei. The DAPI was incubated at RT for 10 minutes. The sections were washed thrice with H<sub>2</sub>O. The slides were dried, and sections were covered with safemount QPath® (VWR™ chemicals, #00647520). Images were taken with ApoTome Zeiss microscope.

### 3.5.3 Adult GBM biopsies

Immunostainings were performed on three different adult tumor samples obtained after resection: T033, T035, T038. Biopsy sections were dried at 60°C in an oven for 1 hour. Slides were soaked with consecutive solutions (Xylene 10 minutes 2 times, EtOH 100% 5 minutes 2 times, EtOH 95%, EtOH 80%, EtOH 75% 2 minutes each). Slides were washed twice with H<sub>2</sub>O for 2 minutes. Antigen retrieval was performed with TRIS-EDTA (pH 9.0, 10 mM Tris base, 1 mM EDTA, 0.05% Tween 20). Biopsies were permeabilized with PBS-T 0.3% (PBS 0.3% tritonX) for 10 minutes. Biopsies were incubated with TrueBlack 1x in EtOH 70% (Biotium, #23007) for 30 seconds each. Blocking was performed with Normal Donkey serum 10% in PBS-1x for 1 hour. Biopsies sections were incubated with primary antibodies (see **table 2**) diluted in PBS containing 1% normal donkey serum overnight at 4°C. The secondary antibodies (see **table 3**) were incubated at RT for 2 hours. DAPI (1/10000, Sigma-Aldrich®, #D9542) was used to color the nuclei. The slides were washed thrice with PBS-1x after each step from the primary antibody step. The DAPI was incubated at RT for 10 minutes. The DAPI was washed with H<sub>2</sub>O thrice. Fluoromount-G™ (Invitrogen, #00-4958-02) was used to mount the slides with coverslips. Images were taken with ApoTome Zeiss microscope.

<b>Primary Antibody</b>	<b>Species</b>	<b>Dilution</b>	<b>Reference</b>
Anti-R-PTP- $\zeta$	Monoclonal Mouse	1/40 (1 $\mu$ g)	BD biosciences®, #610180
Anti-Nestin	Monoclonal Mouse	1/200	Santa Cruz®, #SC23927
Anti-K27M	Monoclonal Rabbit	1/500	RevMab Biosciences®, #31-1175-00
Anti-Sox2	Monoclonal Rabbit	1/200	Cell Signalling Technology®, #3579
Anti-GFAP	Polyclonal Chicken	1/1000	Abcam®, #ab4674
Anti-Iba1	Polyclonal Goat	1/1000	Abcam®, #ab5076

**Table 2: List of primary antibodies used for the immunofluorescence staining.**

<b>Secondary Antibody</b>	<b>Host Species</b>	<b>Dilution</b>	<b>Fluorochrome</b>	<b>Reference</b>
Anti-mouse	Donkey	1/500	Rhodamine Red™-X	Jackson Immuno-Research, #715-296-150
Anti-mouse	Donkey	1/500	Cy5	Jackson Immuno-Research, #715-175-150
Anti-rabbit	Donkey	1/500	Cy5	Jackson Immuno-Research, #711-175-152
Anti-rabbit	Donkey	1/500	FITC	Jackson Immuno-Research, #711-095-152
Anti-chicken	Donkey	1/500	Cy5	Jackson Immuno-Research, #703-175-155
Anti-goat	Donkey	1/500	Cy5	Jackson Immuno-Research, #705-175-147

**Table 3: List of secondary antibodies used for the immunofluorescence staining.**

### 3.6 Quantitative RT-PCR

The RNA extraction was performed with Nucleospin RNA kit (MACHEREY-NAGEL, #740955.50). The RNA quantities were evaluated with a Nanodrop 2000 (ThermoScientific™, #ND-2000). The RNAs were retro-transcribed using ProtoScript II kit (New England Biolabs, #E6560S) and a Sensoquest Labcycler. The cDNA product was used for quantitative real-time (RT) PCR in a SYBR Green (Eurogentec, #UF-NSMT-B0101) using the LightCycler 480 (Roche®, #1536). Primer sequences were designed as follows: PTPRZ1 forward: GCTTTGATGCGGACCGATTTT; PTPRZ1 reverse: ACGACTAACACTTTCGACTCCA. Gene expression levels were normalized according to the Ezrin or GAPDH housekeeping genes. Primer sequences were designed as follows: Ezrin forward: TGCCCCACGTCTGAGAATC; Ezrin reverse: CGGCGCATATACAACATCATGG and GAPDH forward: CATGAGAAGTATGACAACAGCCT and GAPDH reverse: AGTCCTTCCACGATACCAAAGT.

### 3.7 Western Blot

For the extraction of proteins, cells were incubated with lysis buffer (NaCl 450 mM, Tris HCl 50 mM, 1% Triton 100x, protease/phosphatase inhibitors 1/100) for 10 minutes on ice. A sonication was performed with a Labsonic U machine. The samples were centrifugated for 10 minutes at 13 000 rpm at 4°C. The supernatants were collected. The proteins quantification was performed with the Bradford method and BSA standard curve. Lecture was performed at 580 nm (Thermo Labsystems Multiskan Ascent).

The electrophoretic migration was performed with 8% gel (H<sub>2</sub>O, Tris 1.5 M (pH 8.8), 0.5 (pH 6.8), acrylamide, SDS 10%, TEMED, APS 10%). The transfer was performed onto a PDVF membrane (Roche, #3010040001). The membrane was incubated in 5mL of milk solution for the blockage step. The membrane was then incubated with primary antibody (1/1000, anti-R-PTP-ζ, Monoclonal Mouse (BD biosciences®, #610180)) in 5 mL of milk solution overnight at 4°C. The membrane was washed thrice with T-TBS (Tris Base, NaCl, H<sub>2</sub>O, pH 7.6) for 5 minutes each and incubated during 1 hour at room temperature with the secondary antibody (1/2000; anti-mouse HRP-linked (Cell Signaling Research, #05/2019)). The membrane was washed thrice with T-TBS (Tris Base, NaCl, H<sub>2</sub>O, pH 7.6) for 5 minutes each. After incubation with HRP-conjugated antibody, the chemiluminescent signal was recorded using the chemiluminescent substrate (Thermofisher, SuperSignal™ West Pico PUS

Chemiluminescent Substrate, #34577) and the western blot imaging system (Cytiva, amersham ImageQuant 800). For the charge control, the membrane was incubated with the  $\beta$ -Actin peroxidase (1/10 000 (Sigma-Aldrich, #A3854-200UL)) during 1 hour at RT. Again, chemiluminescent signal was recorded using the chemiluminescent substrate (Thermofisher, SuperSignal™ West Pico PUS Chemiluminescent Substrate, #34577) and the western blot imaging system (Cytiva, amersham ImageQuant 800).

### **3.8 Cell Viability Assay**

For cell viability assays, cells were seeded at a density of 1000 cells in 90  $\mu$ l of NPC medium per well in a 96-well plate. Cells were treated with different concentrations (100  $\mu$ M, 30  $\mu$ M, 10  $\mu$ M, 3.3  $\mu$ M, 1.1  $\mu$ M, 0.37  $\mu$ M, 0.12  $\mu$ M) of NAZ2329 (MedChemExpress, HY-103693) diluted in DMSO. The incubation period was 6 days. To assess the viability of the cell, a CellTiter Glo 2.0 kit was used. The CellTiter glo reagent was added to the plate (25  $\mu$ l/well). Bioluminescence was analyzed by a luminometer (TRISAR<sup>2</sup>S LB942 Multimode Reader, Berthold Technologies). The setting of the luminometer was 2 minutes of shaking the plate and reading of all the wells for 20 minutes.

Another viability assay was performed in 12-well plates, 10 000 cells were seeded in 1mL of NPC medium. Cells were treated with 100  $\mu$ M of NAZ2329 (MedChemExpress, HY-103693) or 99,99% DMSO for 6 days. The number of living cells were counted after the 6 days. The medium containing the cells was recover and centrifugated for 3 minutes at 6000 rpm. The supernatant was thrown away and the cells were dissociated in 200  $\mu$ l of accutase (StemCell Technologies™, #07922) for 5 minutes. The cells were resuspended with 1ml of PBS and centrifugate for 3 minutes at 6000 rpm. The supernatant was thrown away and the cells were resuspended in 50  $\mu$ L of PBS. The cells were counted in trypan blue with the Countess™ 3 FL Automated Cell Counter (Invitrogen™, #AMQAF2000)

### **3.9 Migration Assay**

The migration assay was performed in 96-well chemotactic chamber with 10  $\mu$ m pore with a well capacity of 30  $\mu$ L (Neuro Probe, #SKU: 106-10). The bottom chambers were filled with 30  $\mu$ L of medium-free DMEM containing 5% of FBS. In the upper chamber, four different cell lines (KNS42, Res259, DIPG007, DIPG012) were seeded at a density of 20 000 cells by well in DMEM medium (for KNS42 and Res259 cell lines) or NPC medium (for DIPG007 and DIPG02 cell lines). All the cells were treated with different concentrations of NAZ2329 (100

$\mu\text{M}$ , 30  $\mu\text{M}$ , 10  $\mu\text{M}$ , 3.3  $\mu\text{M}$ , 1.1  $\mu\text{M}$ ) (MedChemExpress, HY-103693). There were 2 conditions per cell line: a condition with only the treatment to NAZ2329 and another condition with the treatment to NAZ2329 together with Pleiotrophin 100 ng/ml (R&D systems, #252-PL-050).

After 18 hours of incubation in a 5%  $\text{CO}_2$  humidified incubator at 37 °C, cells having migrated in the lower chambers were fixed with 4% paraformaldehyde (PFA) for 15 minutes and rinsed thrice with PBS-1x. The cells were stained with Violet crystal solution (Violet crystal 10% in EtOH 95%). The chemotactic chambers were washed with deionized water. The chemotactic chambers were dried and fixed on slide with safemount QPath® (VWR™ chemicals, #00647520).

### **3.10 Statistical analysis**

Quantitative data are expressed as mean  $\pm$  SEM of a minimum of three biologically independent experiments and analyzed by GraphPad Prism 8®. Kruskal-Wallis tests have been performed and a p-value of  $< 0.05$  was considered as statistically significant.

---

# RESULTS

---

## 4 Results

### 4.1 Expression of PTPRZ1 in glioma cell lines

The different glioma cell cultures (Res259, KNS42, T013, DIPG007 and DIPG012) were cultivated in T75 flasks. At different passages, the cells were collected and preserved as a dry pellet at -20°C. To perform the analysis of *PTPRZ1* expression, the total RNA was isolated from each sample using a Nucleospin RNA kit.

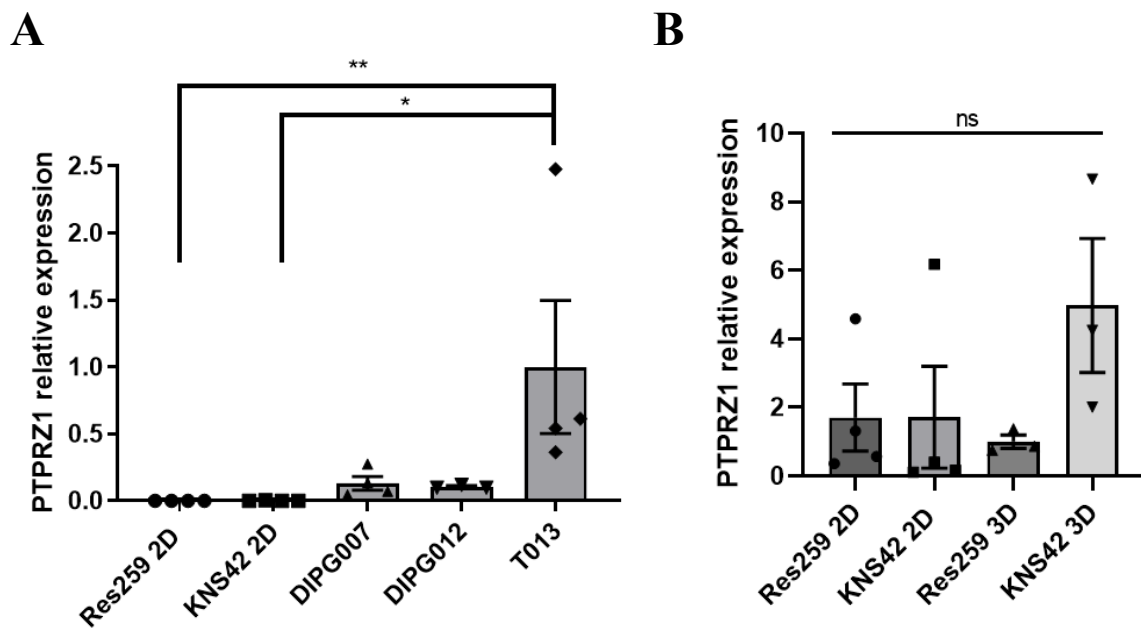


**Figure 10: *PTPRZ1* is expressed in different gliomas cell lines.** (A) qPCR showed higher *PTPRZ1* expression in adult glioblastoma T013 cell line compared to the pediatric cell lines. (N=4) Results are displayed as Mean ± SEM and were analyzed with Kruskal-Wallis test (p-value = 0.0034, \*\* = 0.0069, \* = 0.0167). (B) qPCR showed similar expression in Res259 and KNS42 cell lines when cultured in adherence (2D) or as spheres (3D). (N=3) Results are displayed as Mean ± SEM and were analyzed with Kruskal-Wallis test (ns = not significant)

The analysis of *PTPRZ1* expression by RT-qPCR reveals detectable RNA levels in the 5 different cell lines. *PTPRZ1* seems to be more expressed in the T013 adult glioblastoma cell line. Among pediatric glioma cell lines, DIPG007 and DIPG012 show intermediate expression, whereas Res259 and KNS42 cells have almost undetectable expression (**Figure 10A**). The Kruskal-Wallis statistic test shows a statistically significant difference between Res259 2D and T013 (\*\*, p-value = 0,0069) and a significative difference between the KNS42 2D and T013 (\*, p-value = 0,0167).

We also confirmed that *PTPRZ1* expression was not increased when Res259 and KNS42 were cultured as 3D spheres in NPC medium (**Figure 10B**).

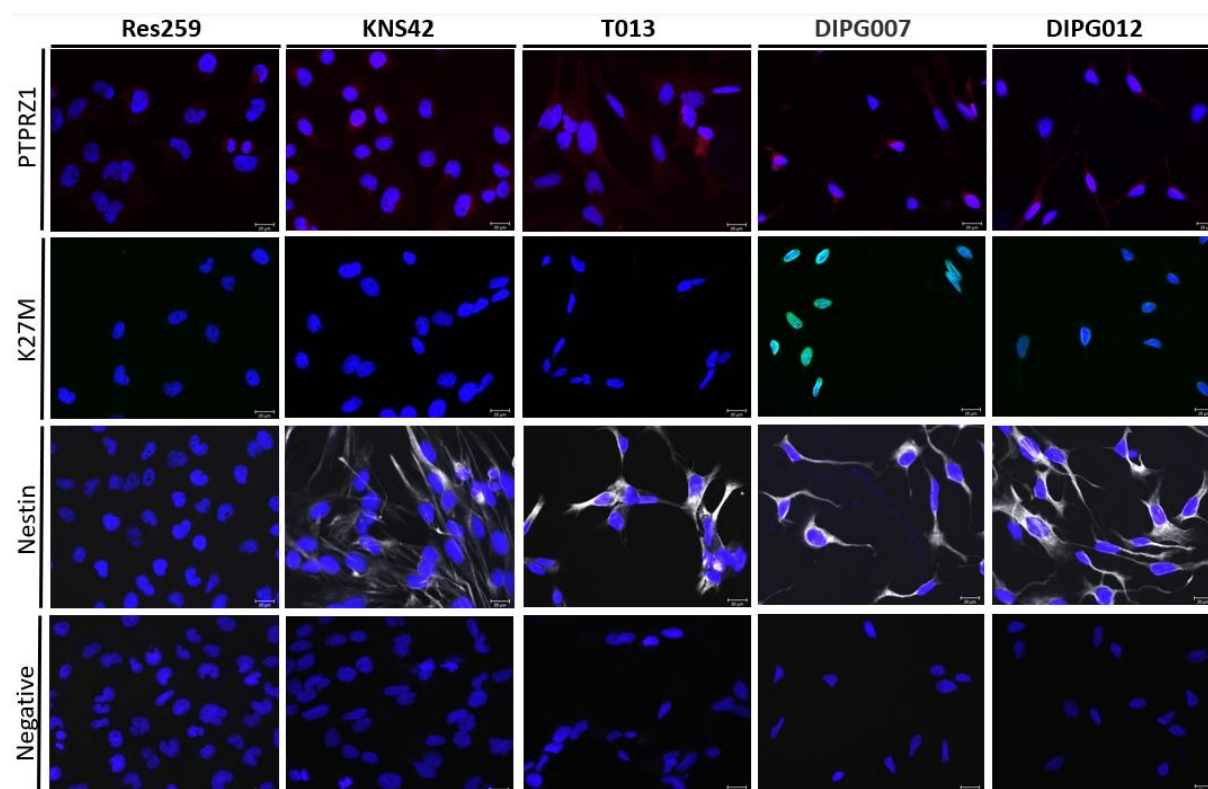


**Figure 11: Immunofluorescent staining of cell lines on coverslips.** Blue staining corresponds to DAPI, red staining corresponds to *PTPRZ1*, green staining corresponds to the mutation K27M, and white staining corresponds to Nestin. (Scalebar = 20 µm)

The different cell lines were cultivated on coverslips to allow an immunofluorescent staining on adherent cells. Immunofluorescent staining was performed to confirm the presence of *PTPRZ1*. The immunofluorescence showed very low *PTPRZ1* expression in the cytoplasm of the different lines (**Figure 11**).

We also used immunofluorescent staining to characterize the expression of classical GBM and DIPG markers in the different cell lines we have used. The H3 K27M mutation is described as specific to DIPG tumors. In the cell lines, the staining indeed showed the K27M mutation in DIPG007 and DIPG012 cells as described in the literature (**Figure 11**). The Nestin protein (highly expressed in high-grade glioma cells and stem-like cells) was identified in the KNS42, T013, DIPG007 and DIPG012 cell lines. Nestin was not identified in the Res259 cells (**Figure 11**).



Previous results obtained with mass spectrometry in the host lab show that the PTPRZ1 protein was identified on the T013 adult GBM cells culture as neurospheres, but less abundant upon dissociated culture (data not shown). We therefore performed an immunofluorescent staining on neurosphere sections to confirm those results.

This immunofluorescent staining showed indeed a stronger expression of PTPRZ1 at the plasma membrane (**Figure 12**). In these neurospheres configurations, the cells also express stem-cell associated markers such as Sox2 and Nestin (**Figures 12 and 13**). This immunostaining again showed the presence of Nestin in the different cell cultures (**Figure 13**).

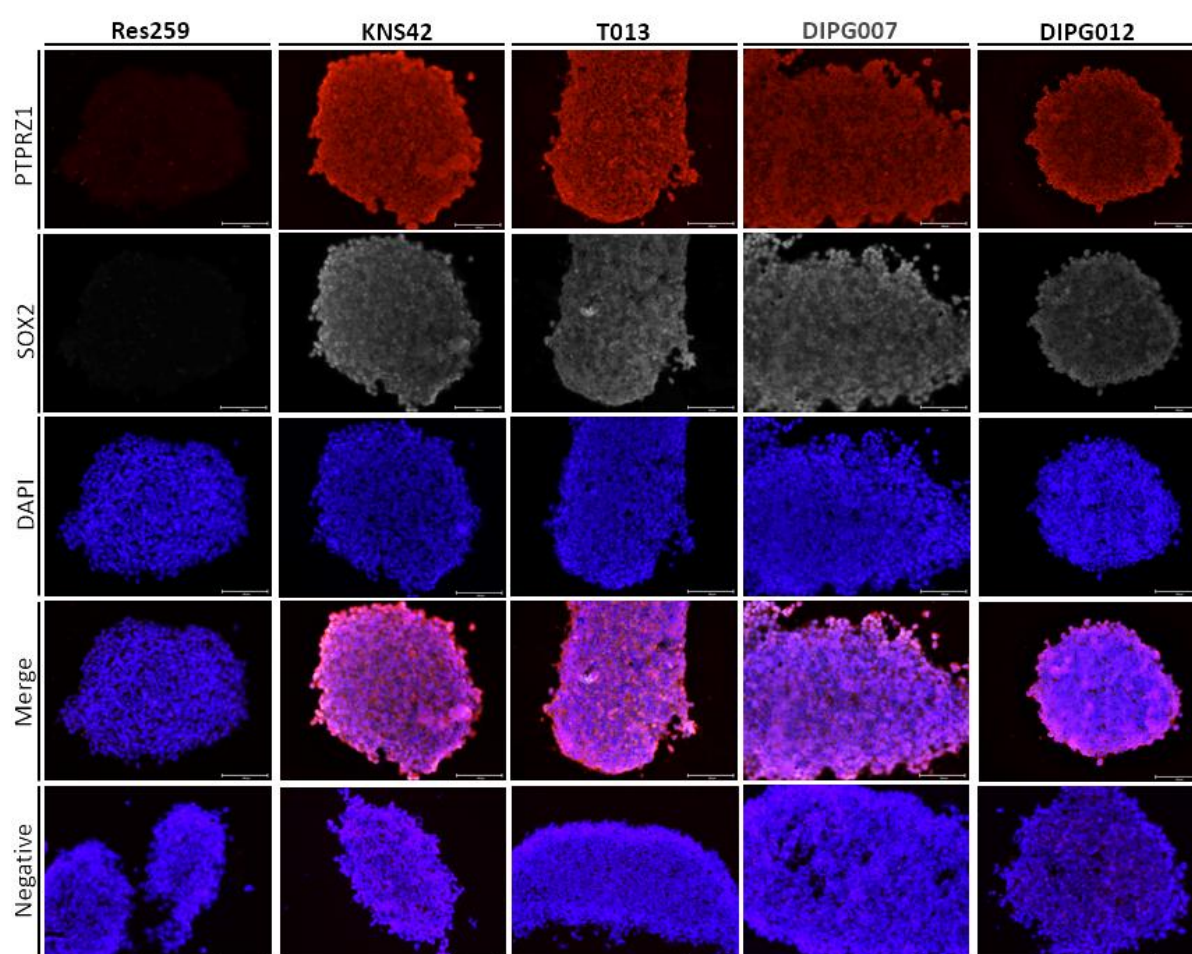


**Figure 12: Immunofluorescent staining of cell lines on neurospheres.** Blue staining corresponds to DAPI, red staining corresponds to PTPRZ1, and white staining corresponds to Sox2.

Higher magnification shows with more details the staining of PTPRZ1, Sox2 and Nestin. We can observe that proteins such as PTPRZ1 and Nestin are at the cytoplasmic membrane, while the Sox2 protein is at the nucleus (**Figure 14**).

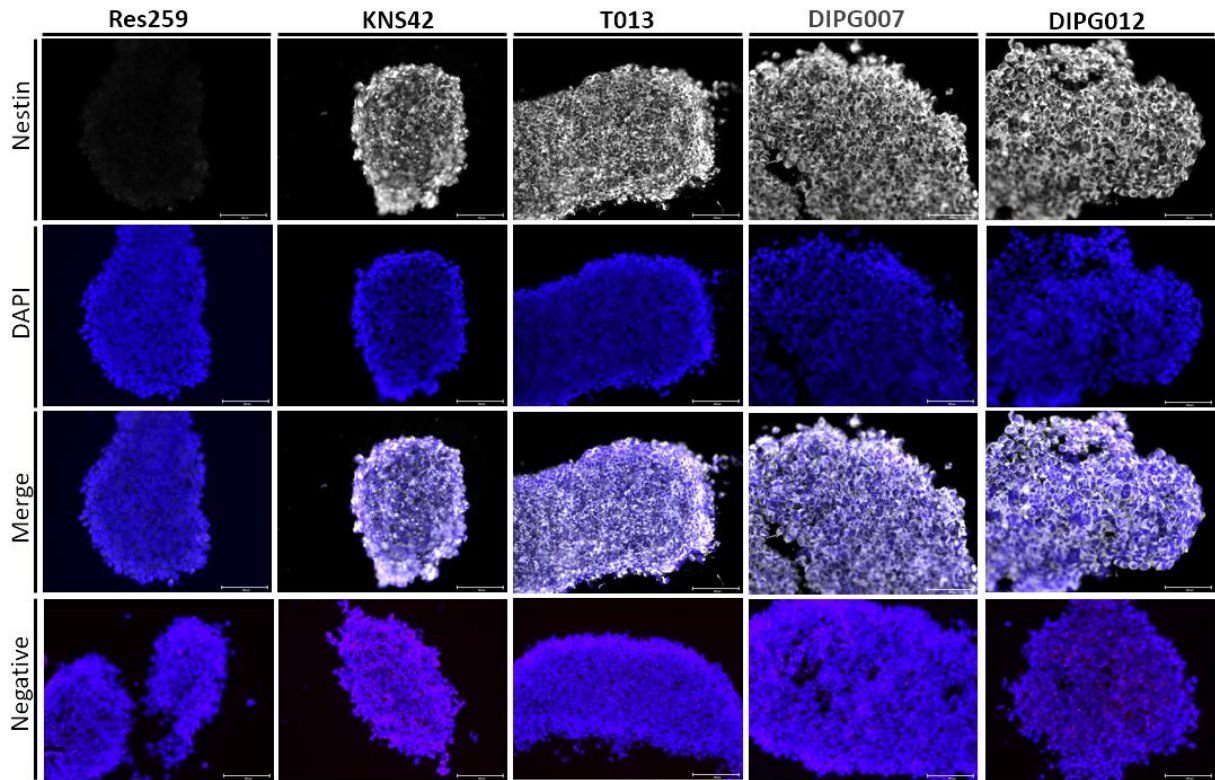


**Figure 13:** Immunofluorescent staining of cell lines on neurospheres. Blue staining corresponds to DAPI, white staining corresponds to Nestin.

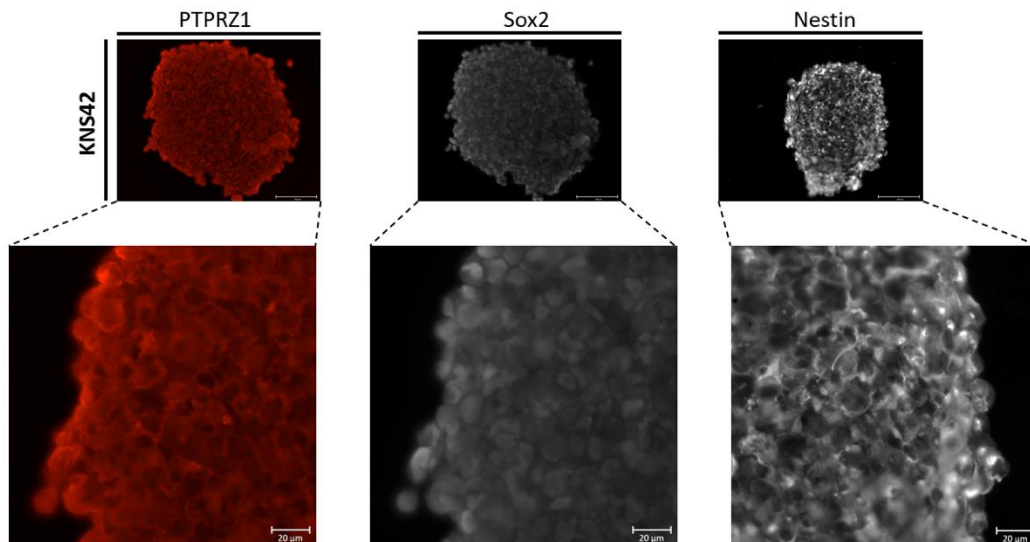


**Figure 14:** Higher magnification of immunofluorescent staining of cell lines on neurospheres. PTPRZ1 and Nestin proteins appear at cytoplasmic membrane while Sox2 protein is at the nucleus.

## 4.2 Expression of different isoforms of PTPRZ1

To confirm the presence of PTPRZ1 in the different cell cultures, a Western Blot has been performed on total proteins extracted from each culture. This experiment should confirm the results from the qPCR experiments and demonstrate the presence of PTPRZ1 as previously identified. According to the literature, the PTPRZ1 protein can be present under different isoforms with different molecular weights. This experiment was therefore conducted to provide information about the possible presence of different isoforms.

We indeed observed different signals at various molecular weights in the different cell lines. For the cell lines KNS42 2D/3D and Res259 2D/3D, we observed a signal at a molecular weight of ~120 kDa, which appears stronger when cells are cultivated in adherent conditions. For the adult cell lines T013 and the two DIPG cell lines (DIPG007 and DIPG012), we observed few signals at different molecular weights. There are signals at ~80 kDa and other signals from ~250 kDa and above (**Figure 15**).

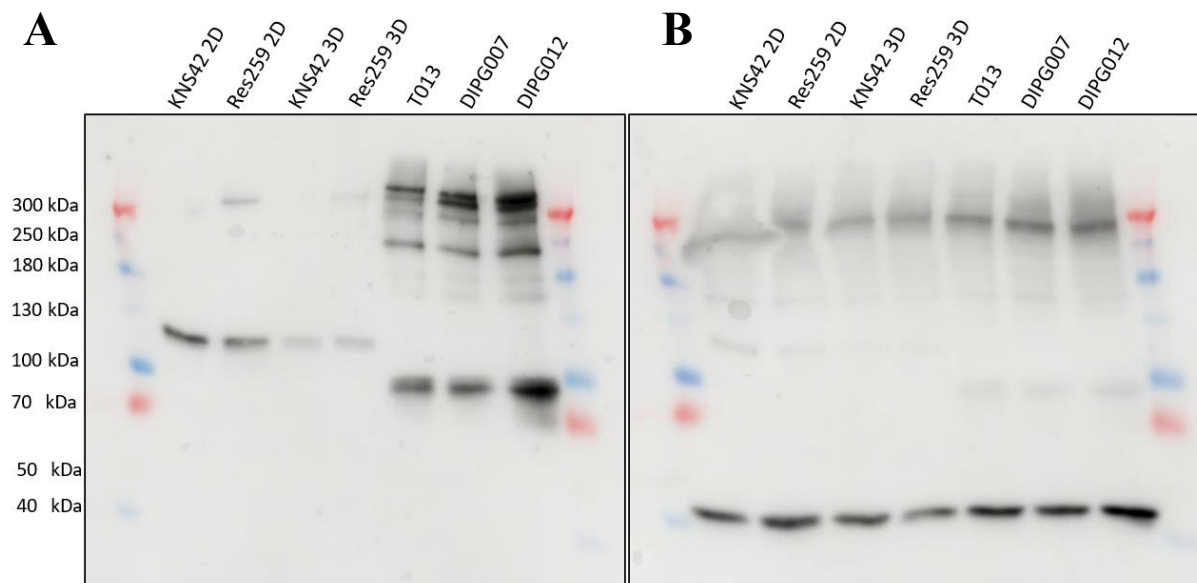
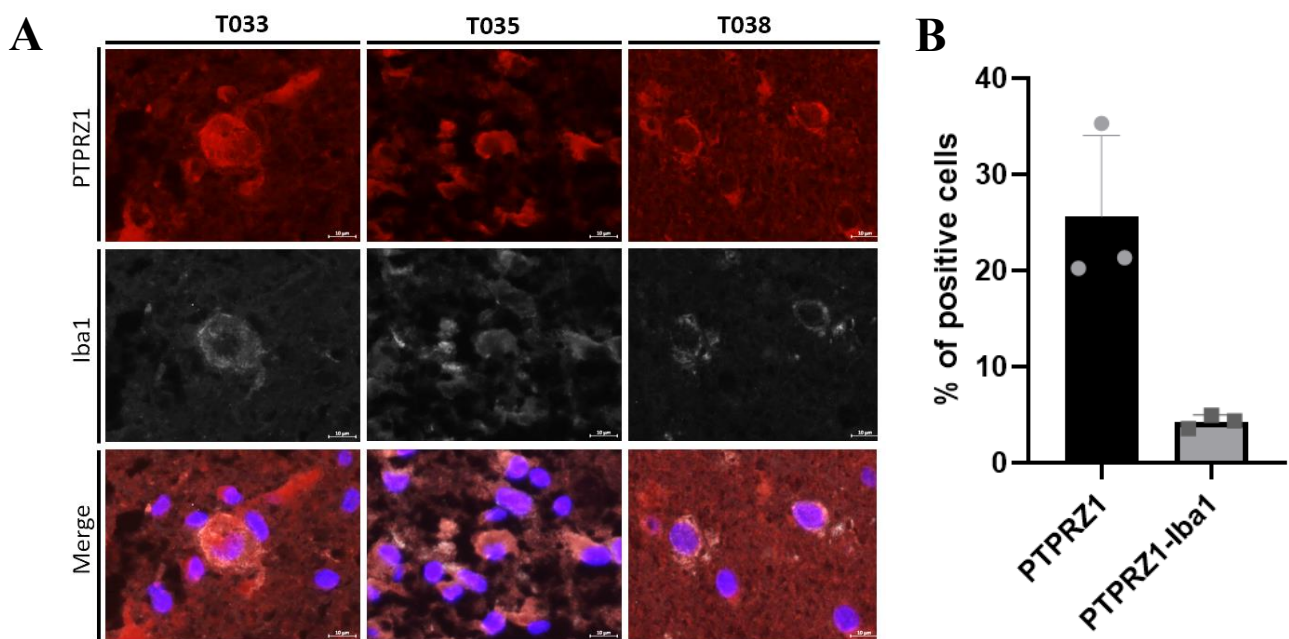


**Figure 15: Expression of different isoforms of PTPRZ1.** (A) Western Blot analyses of PTPRZ1 in different pediatric cell lines (KNS42, Res259, DIPG007, DIPG012) and adult cell line (T013). Proteins extractions were performed on 2D and 3D cells of KNS42 and Res259. (n=1) (B)  $\beta$ -actin (42 kDa).

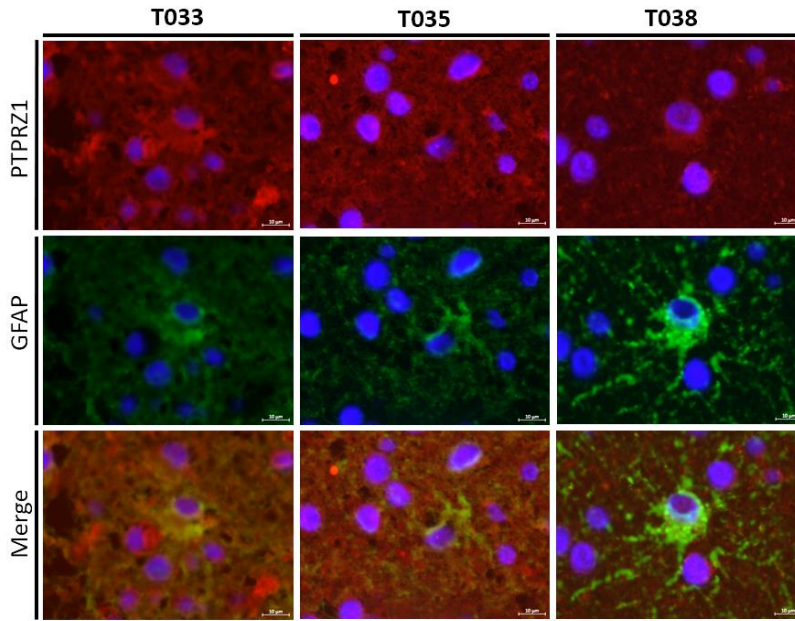


### 4.3 Expression of PTPRZ1 in adult GBM tissue

PTPRZ1 has been identified in the different pediatric cell cultures *in vitro*. To further investigate, we wanted to look at the expression of PTPRZ1 in freshly resected tumor tissue. However, this investigation could not be performed on pediatric glioma tissues due to the scarcity of available pediatric samples. The immunofluorescence staining has been done on adult biopsies. The results show the presence of PTPRZ1-positive cells in the tissue of 3 different adult GBM samples (T033, T035, T038). To define which cell types inside the tumor are expressing PTPRZ1, co-stainings have been performed for detection of Iba1 (expressed by microglia) and GFAP (expressed by astrocytes). The colocalization staining shows the presence of cells expressing both PTPRZ1 and Iba1 (**Figure 16A, B**) as well as a few cells expressing both PTPRZ1 and GFAP (**Figure 16C, D**).



C



D

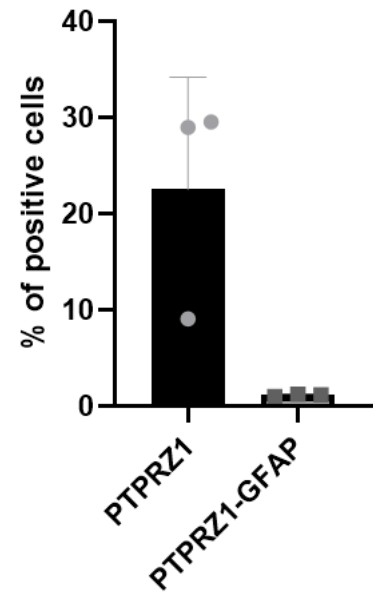


**Figure 16: Immunofluorescent staining of biopsies.** (A) Blue staining corresponds to DAPI, red staining corresponds to PTPRZ1, white staining corresponds to Iba1. (B) Percentage of positive-cells for PTPRZ1 and PTPRZ1-Iba1. (C) Blue staining corresponds to DAPI, red staining corresponds to PTPRZ1, green staining corresponds to GFAP. (D) Percentage of positive-cells for PTPRZ1 and PTPRZ1-GFAP.

## 4.4 Effect of NAZ2329 on PTPRZ1 function

The aim of this experiment was to look for the effects of PTPRZ1 inhibition (using the small molecule NAZ2329) on cell viability and sphere formation. We thus cultivated various GBM cell lines with a single concentration of the inhibitor (100  $\mu$ M) or the vehicle (DMSO). The experiment shows a decrease in the sphere number in presence of NAZ2329 compared to DMSO. NAZ2329 (applied at 100  $\mu$ M) seems to affect all cell lines (**Figure 17A**). Cell counting shows a sharp decrease in living cells in presence of NAZ2329 100  $\mu$ M compared to cells in presence of DMSO (**Figure 17B**).

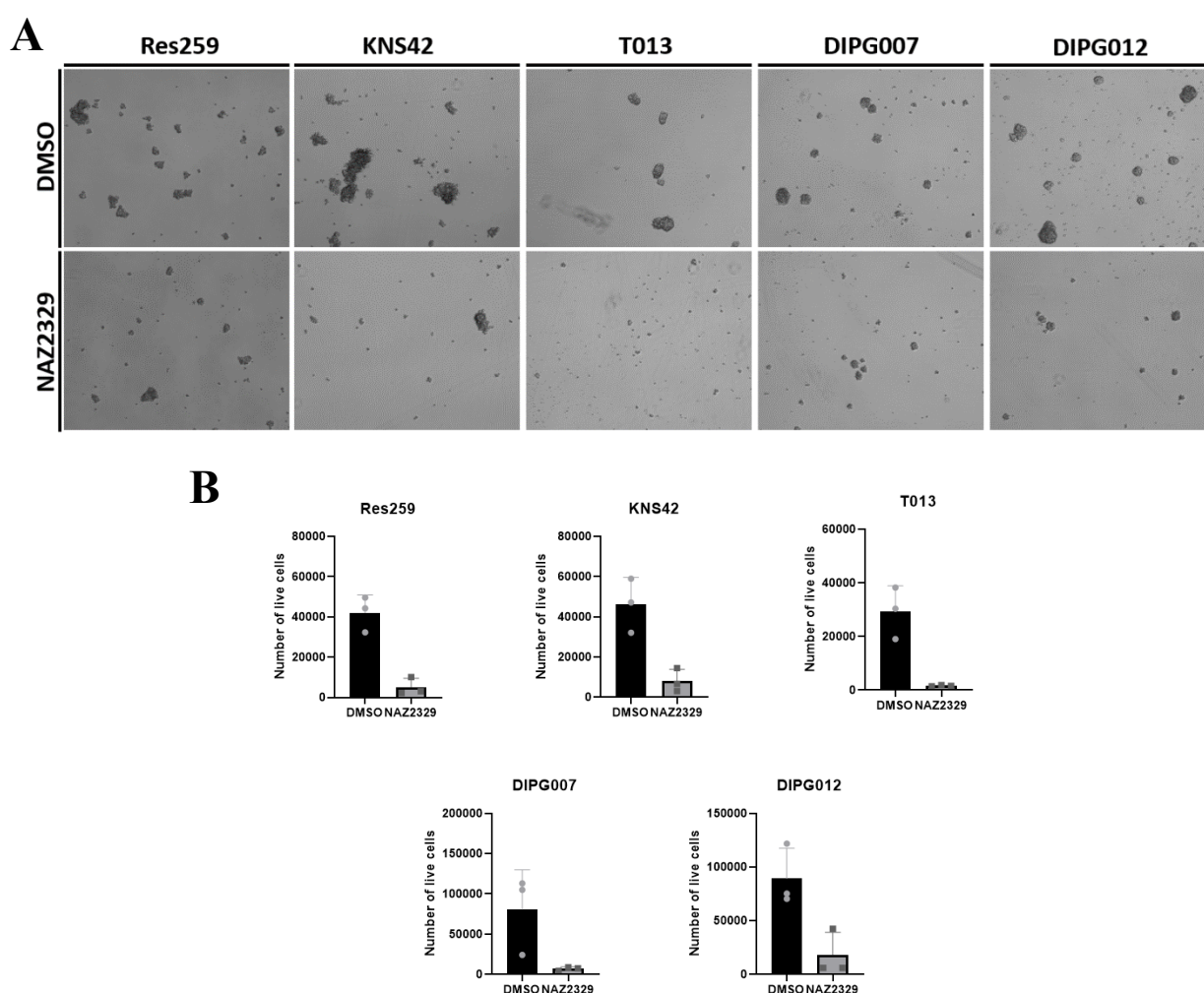


**Figure 17: Sphere formation and cell viability in presence of NAZ2329.** (A) Cells were seeded in 12-well plates in NPC medium during a 6 days incubation period in presence of NAZ2329 or DMSO. Images represent the five cell lines. (B) The bar graphs show the number of living cells per well in presence of DMSO or NAZ2329 after 6 days. (n=3)

Based on the observation that NAZ2329 apparently influences sphere formation and cell viability, we wanted to get a closer look at the effects of this PTPRZ1 inhibition on cell proliferation.

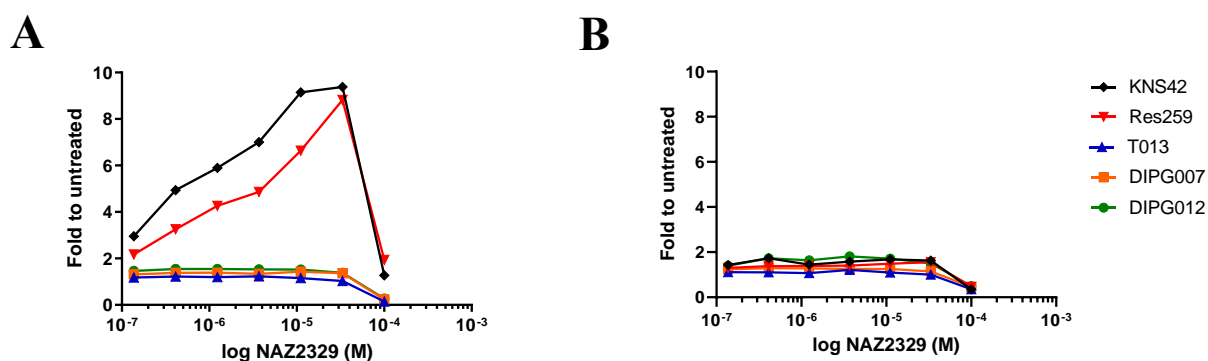


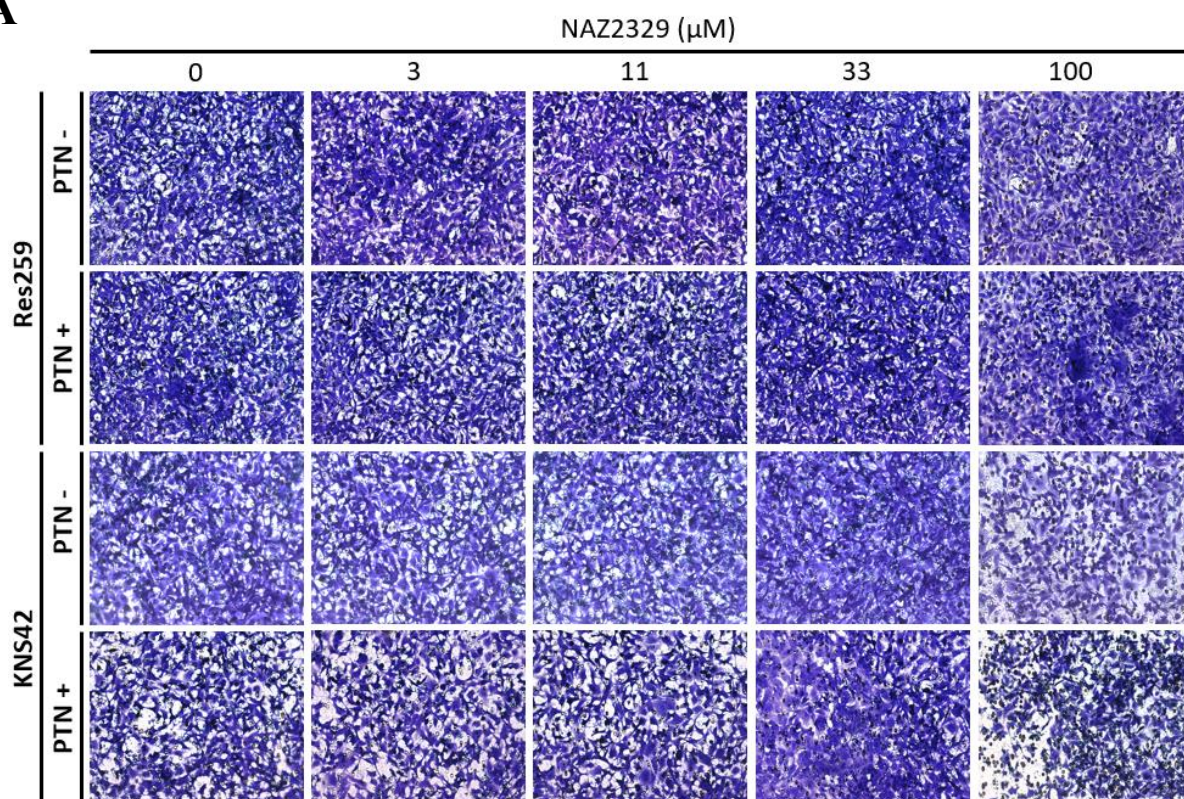
**Figure 18: Effect of NAZ2329 on PTPRZ1.** (A,B) The plots show the effect of NAZ2329 at different concentrations on the different cell lines after a 6 days incubation period with NAZ2329. DIPG007 and DIPG012 cells increase in a concentration-dependent manner. Plot A represents the n1 (left) and B represents n2 (right).

We verified the effects of different concentrations of NAZ2329 on cell proliferation with a Cell Titer Glo 2.0 kit. In 96-well plate, 1000 cells/well of each cell culture were seeded in NPC medium with dilution series of NAZ2329 for 6 days of incubation. The first plot represents the first experiment (**Figure 18A**). It shows that NAZ2329 increased cell proliferation on two different cell lines (DIPG007, DIPG012) in a concentration-dependent manner. For the three other cell lines, NAZ2329 did not appear to influence the cell proliferation. These results also show that the viability of cells drastically decreases at 100  $\mu$ M. We repeated this experiment but did not observe the same effect of NAZ2329 on DIPG007 and DIPG012 anymore (**Figure 18B**).

As mentioned previously in the introduction, PTPRZ1 is a receptor that could be implicated in the migration of the glioma cells. This migration could be influenced by the interaction of the receptor with its ligand, pleiotrophin. A migration assay was performed to observe the potential effect of the pleiotrophin on cells in presence or absence of NAZ2329.

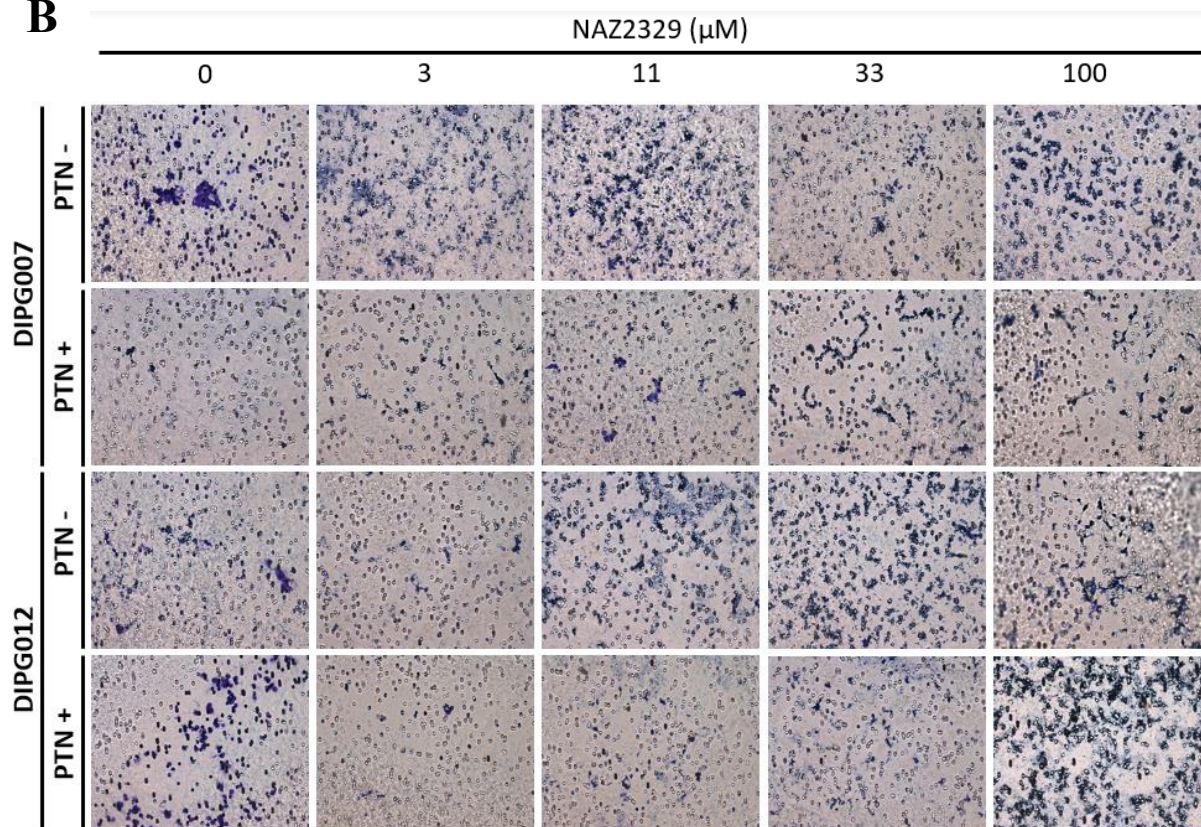


A



The migration assay does not show important differences in the migration in presence of different concentrations of NAZ2329 for Res259 and KNS42 cell lines after a 18 hours period of migration. The cells have considerably migrated in all different conditions for the two adherent cell lines (**Figure 19A**). There is no difference between the presence or the absence of pleiotrophin. Conversely, the two other cell lines DIPG007 and DIPG012 barely migrated, in all the different conditions (**Figure 19B**).



**B**

**Figure 19: Cells migration in presence of NAZ2329 and in presence or not of pleiotrophin.** Representative pictures of in vitro Boyden chemotaxis chamber migration assay reflecting the different migration phenotype. (A) Adherent cell lines Res259, KNS42. (B) 3D cell lines DIPG007, DIPG012.

---

# DISCUSSION

---

## 5 Discussion

---

The main objective of this work was to study the expression of *PTPRZ1* in different pediatric and adult glioma cell cultures, and assess its role in cell proliferation and migration, with the ultimate purpose of assessing the potential of this protein for targeted therapies in glioma patients.

The expression of *PTPRZ1* in the different cell cultures was first identified by RT-qPCR. These results suggest that *PTPRZ1* seems to be more abundant in the adult glioblastoma cell line T013, but also demonstrates a relevant expression of *PTPRZ1* in DIPG007 and DIPG012 cultures. In comparison, Res259 (pediatric low-grade glioma) and KNS42 (pediatric high-grade glioma) cells only display minor expression of *PTPRZ1*. Given that these cells are cultured in adherence, we aimed to verify whether the cell culture conditions have an impact on *PTPRZ1* expression. Results do not highlight any modification of *PTPRZ1* expression once Res259 and KNS42 cells are cultivated in 3D. However, the variability is high among replicates. To perform the RT-qPCR, the RNA has been extracted from dry cell pellets collected at different passages. The cells were cultured in 3D spheres. The sphere number and size were not standardized, which could partly explain the expression variability. This experiment should be repeated with seeding the same number of cells and applying the same incubation time before collection.

The expression of *PTPRZ1* has been confirmed using immunofluorescence. This technique gives important information regarding the localization of the protein. Our results show the localization of the protein at the plasma membrane. Alongside, characterization of the different pediatric cell lines has been done. Sox2 and Nestin are known as stem cell markers<sup>7</sup>. We found that, except for the low-grade Res259 cell line, all the pediatric and adult HGGs show an expression of these two stem cell markers in addition to the *PTPRZ1* expression. This information brings up the thought that the cells expressing *PTPRZ1* may be related to a stemness character.

Immunofluorescent staining does not provide quantitative information about the expression of the protein. Another technique that could be used is the flow cytometry. This could have been interesting to compare the data from RT-qPCR and the flow cytometry to confirm the expression of *PTPRZ1* at the cell membrane in a quantitative manner (proportion of positive cells and “intensity” of expression).

As previously mentioned, PTPRZ1 can be present under different forms: long, short, and soluble<sup>70</sup>. However, the immunofluorescence technique and the choice of primary antibody, even though it is a monoclonal antibody, do not give any information regarding the isoforms present at the cytoplasmic membrane. Indeed, the primary antibody targets the intracellular phosphatase domain of PTPRZ1, which is present on all protein isoforms<sup>79</sup>. We therefore conducted a western blot analysis to reveal the presence of different isoforms of the protein.

For the T013 adult cell line as well as DIPG007 and DIPG012 pediatric cell lines, we can observe a signal at ~250 kDa that could be the short form (PTPRZ1-B) of PTPRZ1. For these three cell lines, we can also notice the presence of signals at ~300 kDa and more. These signals could correspond to the long form of PTPRZ1 (PTPRZ-A) at ~380 kDa<sup>79,80,85</sup>. Note that the amount of chondroitin sulfate chains on PTPRZ1 may slightly modify its molecular weight, therefore shifting the signals on the western blots, and this could vary depending on the experimental conditions. In these cell lines, there is also the presence of signal at ~80 kDa. The signal could be an intracellular fragment cleaved by  $\gamma$ -secretase<sup>74</sup>.

Indeed, Chow et al demonstrated that the different long or short isoforms of PTPRZ1 could be cleaved by metalloproteinase, which releases extracellular fragment (ECF) or by  $\gamma$ -secretase, which releases intracellular fragment (ICF)<sup>74</sup>. As mentioned before, the primary antibody used targets the intracellular fragment of PTPRZ and therefore, the signals cannot be an extracellular fragment of the receptor. Interestingly, adult T013 cell line and the two DIPG cell lines (DIPG007 and DIPG012) have the same profile of signal.

In KNS42 and Res259 cell lines (respectively pediatric high- and low-grade glioma), there is no signal at 250 kDa, but there is a presence of signals at ~120kDa. We are still questioning the origin of these signals, given that it does not specifically correspond to a known protein fragment, and considering that the previous experiments (qPCR and immunofluorescence) demonstrated very low expression of PTPRZ1 in the Res259 cell line.

Yamanoi et al published an article about the different isoforms of PTPRZ1. In their article, they described the soluble form of PTPRZ1 as a potential biomarker of glioblastoma's severity, detected in the cerebral spinal fluid (CSF) of patients<sup>86</sup>. It would then be interesting to collect CSF from mice implanted with the various glioma cells and assess whether PTPRZ1 could be a positive pediatric biomarker.

We also aimed to look whether PTPRZ1-expressing cells are expressed in freshly resected tumor tissue. Given the low availability of pediatric glioma tissues, we could only perform the staining on adult samples. We observed PTPRZ1-positive cells in the tumors of three different patients.

Our immunostaining on adult biopsies shows the presence of PTPRZ1-positive cells. Interestingly, the investigation to define which cell types inside the tumor express the protein of interest shows colocalization with Iba1 and, to a lesser amount, GFAP. These co-stainings indicate the co-expression of PTPRZ1- and Iba1, putatively on microglial or macrophagic cells. It has already been described in the literature that Iba1+ cells colocalized with GSCs expressing PTPRZ1<sup>87</sup>. The co-expression of PTPRZ1 and GFAP is very slight. Of note, there are also PTPRZ1+ cells that did not express Iba1 or GFAP.

All the images were taken with ApoTome Zeiss AxioImager (epifluorescence microscope). It could thus be interesting to use the Z-stacking with a confocal microscope to confirm that cells appearing positive for PTPRZ1 express also Iba1. In addition, staining of the pleiotrophin would probably provide supplementary information regarding the specificity of the immunofluorescence staining of the receptor.

According to Knudsen et al, the expression of PTPRZ1 is upregulated in the recurrent glioblastoma compared to primary glioblastoma<sup>87</sup>. Interestingly, this upregulation of PTPRZ1 is also observed in breast cancer cells after chemotherapy treatment<sup>88</sup>. Again, it would be interesting to compare the proportion of PTPRZ1 expression in primary tumor biopsy and recurrent biopsy.

In 2017, Shi et al published an article about the tumors-associated macrophages (TAMs) secreting pleiotrophin to increase tumor growth through PTPRZ1. Their hypothesis is that the disruption of the pleiotrophin/PTPRZ1 axis could impede tumor growth<sup>89</sup>. Physiologically, the endogenous ligand pleiotrophin once binding to PTPRZ1 generates the dimerization of the receptor, which results in the inactivation of its phosphatase activity<sup>68</sup>. Therefore, such inactivation enhances consecutively the phosphorylation status of downstream signaling pathways such as ALK, beta-catenin, Fyn (which is a member of the Src family), p190Rho-GAP or beta-adducin, which are known to be involved in cell migration and proliferation<sup>90,91</sup>. During their studies, Shi et al. demonstrated that the use of a specific antibody against PTPRZ1, which impedes the PTPRZ1 inhibition by PTN, induces a decrease of tumor growth and increase the survival rate. They also demonstrated that the use of this specific anti-PTPRZ1

prevents the phosphorylation of AKT protein. Whereas in absence of anti-PTPRZ1 and stimulation with rhPTN, there is detection of phosphorylated Akt as well as SFK (Src family kinases)<sup>89</sup>. Unfortunately, Shi et al. do not describe the mechanism of action of the antibody against PTPRZ1, which could have brought more value to the experiments.

Fujikawa et al. have developed a phosphatase allosteric inhibitor (NAZ2329) with good specificity for PTPRZ1, which they showed as an inhibitor of viability in glioma cell lines<sup>84</sup>. NAZ2329 inhibits the catalytic activity of the receptor by preventing the enzymatic hydrolysis between arginine side chain and phosphate group of the substrate<sup>84</sup>. We performed viability/proliferation assays with this small molecule inhibitor. By applying a high concentration of the molecule, we observed that sphere formation was drastically decreased, as well as the number of living cells. Those results were suggesting that PTPRZ1 has a role in the sphere formation and viability.

Another experiment has been performed to assess functionality of NAZ2329. To reach that goal, we applied a Cell Titer Glo assay to measure the level of cell viability after six days upon NAZ2329 treatment (therefore reflecting both cell viability and proliferation). This assay allowed us to test increasing concentrations of the inhibitor and eventually confirm its effect in a more standardized manner. First, results show a dramatic decrease of cell viability upon treatment with 100  $\mu$ M NAZ2329 in all test cell lines, suggesting that the aforementioned decrease in sphere formation capacity was likely due to a toxic effect. The first experiment we performed shows that inhibitor NAZ2329 does not modulate the cell viability of Res259 (pediatric low-grade glioma), KNS42 (pediatric high-grade glioma), and adult T013 glioblastoma cells. Very interestingly, in a first experiment, the cell viability in DIPG007 and DIPG012 increases in a concentration-dependent way, suggesting that the inhibition of PTPRZ1 may actually stimulate cell proliferation of these two cell lines.

The result of this experiment stimulates the discussion regarding the way the receptor and the inhibitor NAZ2329 work, and regarding the fact that Fujikawa et al. do not observe the same effect on GBM cell lines with the use of NAZ2329. Indeed, they observed a decrease in cell proliferation with the use of NAZ2329, as already mentioned<sup>84</sup>. The hypothesis is that, as it is the case for PTN, the inhibition by NAZ2329 of the receptor prevents tyrosine dephosphorylation of various intracellular proteins and thus, enhances the phosphorylation of signaling pathways previously recruited and implicated in the cell proliferation. Aside of PTPRZ1 inhibition, many signaling pathways may contribute to regulating the cell

proliferation. Depending on the cellular model and the biological context, these pathways can be differentially activated, which may explain that NAZ2329 treatment impacts cell proliferation<sup>84</sup>, or does not impact it (as observed in our results). This hypothesis would explain the results obtained with the first experiment of CellTiter Glow assay. Moreover, in their article, Fujikawa et al. showed that NAZ2329 as well as PTN allowed differentiation of oligodendrocyte precursor cells to mature oligodendrocyte<sup>84</sup>, which reinforces the idea that NAZ2329 inhibits the phosphatase activity of the receptor like PTN. The inhibition of the phosphatase activity could enhance phosphorylation status of different substrates, such as AKT, as mentioned in the article of Shi et al<sup>89</sup>, and therefore explain the increased proliferation observed in the experiment. Again, we must keep in mind that the phosphorylation of these substrates can be induced by various growth factors or stimulations, leading to various effects whose nature depends on these growth factors. PTPRZ1 inhibition may only partially contribute to AKT phosphorylation.

This hypothesis could also explain why we could not observe similar results when we repeated this experiment. In this replicate experiment, the proliferation did not increase in a concentration-dependent way for DIPG007 and DIPG012 cell lines. However, only two replicates are not enough to validate or not the observations. The experiment should be repeated several times and rigorously in identical conditions (in order to reproduce the stimulation of phosphorylation of various substrates in the culture) to assess the observation.

In order to verify whether the inactivation of the phosphatase activity of PTPRZ1 by the PTN or NAZ2329 enhances the phosphorylation of several substrates, western blot against phosphorylated protein like Fyn, AKT, beta-catenin should be done. Moreover, Fujikawa et al. used human U251 and rat C6 glioblastoma cell lines, two established cell lines for several years, while we used other cell lines like Diffuse Intrinsic Pontine Glioma DIPG007 and DIPG012, or the adult patient derived T013 glioblastoma cell line. The passage number for these three home-made cell lines is rather low comparing to the passage numbers of U251 or C6 cells.

Another hypothesis is that PTPRZ1 could be implicated in the migration of glioma cells. The migration assay does not show a modulation of migration with the inhibition of PTPRZ1. Moreover, the presence of pleiotrophin does not impact the migration either. It will be interesting to perform the migration assay with different concentrations of pleiotrophin without NAZ2329 to observe a potential difference in the migration. Moreover, Qin et al described a complex of four proteins implicated in the migration of DIPG cell<sup>64</sup>. Assess the expression of

the pleiotrophin, SPARC, SPARCL1, and HSP90B in all cell cultures should be informative for the migration hypothesis.

Ahmadi et al. identify PTPRZ1 as a promising target for therapies using receptors as CAR-T cells for the brain tumor. However, as described earlier, further investigation regarding its mechanism of action is needed to fully understand signaling pathways of the receptor to be able to use it as a potential therapeutic target.



---

# BIBLIOGRAPHY

---

## 6 Bibliography

---

1. Reifenberger, G., Wirsching, H. G., Knobbe-Thomsen, C. B. & Weller, M. Advances in the molecular genetics of gliomas-implications for classification and therapy. *Nature Reviews Clinical Oncology* **14**, 434–452 (2017).
2. Udaka, Y. T. & Packer, R. J. Pediatric Brain Tumors. *Neurologic Clinics* **36**, 533–556 (2018).
3. Weller, M. *et al.* Glioma. *Nature Reviews Disease Primers* **1**, 1–18 (2015).
4. Jiang, Y. & Uhrbom, L. On the origin of glioma. *Upsala Journal of Medical Sciences* **117**, 113–121 (2012).
5. Ostrom, Q. T., Cioffi, G., Waite, K., Kruchko, C. & Barnholtz-Sloan, J. S. CBTRUS Statistical Report: Primary Brain and Other Central Nervous System Tumors Diagnosed in the United States in 2014–2018. *Neuro-Oncology* **23**, III1–III105 (2021).
6. Gupta, M., Djalilvand, A. & Brat, D. J. Clarifying the diffuse gliomas: An update on the morphologic features and markers that discriminate oligodendroglioma from astrocytoma. *American Journal of Clinical Pathology* **124**, 755–768 (2005).
7. Bradshaw, A. *et al.* Cancer Stem Cell Hierarchy in Glioblastoma Multiforme. *Frontiers in Surgery* **3**, 1–15 (2016).
8. Louis, D. N. *et al.* The 2007 WHO classification of tumours of the central nervous system. *Acta Neuropathologica* **114**, 97–109 (2007).
9. Wirsching, H.-G., Galanis, E. & Weller, M. Glioblastoma. in *Handbook of Clinical Neurology* (eds. Berger, M. S. & Weller, M.) vol. 134 381–397 (2016).
10. Louis, D. N. *et al.* The 2016 World Health Organization Classification of Tumors of the Central Nervous System: a summary. *Acta Neuropathologica* **131**, 803–820 (2016).
11. Louis, D. N. *et al.* The 2021 WHO classification of tumors of the central nervous system: A summary. *Neuro-Oncology* **23**, 1231–1251 (2021).
12. Balss, J. *et al.* Analysis of the IDH1 codon 132 mutation in brain tumors. *Acta Neuropathologica* **116**, 597–602 (2008).
13. Turcan, S. *et al.* IDH1 mutation is sufficient to establish the glioma hypermethylator phenotype. *Nature* **483**, 479–483 (2012).
14. Reuss, D. E. *et al.* ATRX and IDH1-R132H immunohistochemistry with subsequent copy number analysis and IDH sequencing as a basis for an “integrated” diagnostic approach for adult astrocytoma, oligodendroglioma and glioblastoma. *Acta Neuropathologica* **129**, 133–146 (2015).
15. Pekmezci, M. *et al.* Adult infiltrating gliomas with WHO 2016 integrated diagnosis: additional prognostic roles of ATRX and TERT. *Acta Neuropathologica* **133**, 1001–1016 (2017).

16. Ludwig, K. & Kornblum, H. I. Molecular markers in glioma. *Journal of Neuro-Oncology* **134**, 505–512 (2017).
17. Arita, H. *et al.* Upregulating mutations in the TERT promoter commonly occur in adult malignant gliomas and are strongly associated with total 1p19q loss. *Acta Neuropathologica* **126**, 267–276 (2013).
18. Molinaro, A. M., Taylor, J. W., Wiencke, J. K. & Wrensch, M. R. Genetic and molecular epidemiology of adult diffuse glioma. *Nature Reviews Neurology* **15**, 405–417 (2019).
19. Weller, M. *et al.* EANO guidelines on the diagnosis and treatment of diffuse gliomas of adulthood. *Nature Reviews Clinical Oncology* **18**, 170–186 (2021).
20. Aldape, K., Zadeh, G., Mansouri, S., Reifenberger, G. & von Deimling, A. Glioblastoma: pathology, molecular mechanisms and markers. *Acta Neuropathologica* **129**, 829–848 (2015).
21. Ostrom, Q. T. *et al.* CBTRUS statistical report: Primary brain and other central nervous system tumors diagnosed in the United States in 2013-2017. *Neuro-Oncology* **22**, IV1–IV96 (2020).
22. Gajjar, A., Reaman, G. H., Racadio, J. M. & Smith, F. O. *Brain Tumors in Children*. (Springer Cham, 2018).
23. Paulsson, A. K., Garcia, M. A., Solomon, D. A. & Haas-Kogan, D. A. Low-Grade Gliomas. in *Brain Tumors in Children* (eds. Gajjar, A., Reaman, G. H., Racadio, J. M. & Smith, F. O.) 223–250 (Springer Cham, 2018).
24. Da-Veiga, M. A., Rogister, B., Lombard, A., Neirinckx, V. & Piette, C. Glioma Stem Cells in Pediatric High-Grade Gliomas: From Current Knowledge to Future Perspectives. *Cancers (Basel)* **14**, 1–18 (2022).
25. Sturm, D., Pfister, S. M. & Jones, D. T. W. Pediatric Gliomas: Current Concepts on Diagnosis, Biology, and Clinical Management. *JOURNAL OF CLINICAL ONCOLOGY* **35**, 2370–2377 (2017).
26. Sturm, D. *et al.* Hotspot Mutations in H3F3A and IDH1 Define Distinct Epigenetic and Biological Subgroups of Glioblastoma. *Cancer Cell* **22**, 425–437 (2012).
27. Zhang, J. *et al.* Whole-genome sequencing identifies genetic alterations in pediatric low-grade gliomas. *Nature Genetics* **45**, 602–612 (2013).
28. Dougherty, M. J. *et al.* Activating mutations in BRAF characterize a spectrum of pediatric low-grade gliomas. *Neuro-Oncology* **12**, 621–630 (2010).
29. Hawkins, C. *et al.* BRAF-KIAA1549 fusion predicts better clinical outcome in pediatric low-grade astrocytoma. *Clinical Cancer Research* **17**, 4790–4798 (2011).
30. Packer, R. J. *et al.* Pediatric low-grade gliomas: Implications of the biologic era. *Neuro-Oncology* **19**, 750–761 (2017).
31. Rakotomalala, A. *et al.* H3.3k27m mutation controls cell growth and resistance to therapies in pediatric glioma cell lines. *Cancers (Basel)* **13**, (2021).

32. Khuong-Quang, D. A. *et al.* K27M mutation in histone H3.3 defines clinically and biologically distinct subgroups of pediatric diffuse intrinsic pontine gliomas. *Acta Neuropathologica* **124**, 439–447 (2012).
33. Bender, S. *et al.* Reduced H3K27me3 and DNA Hypomethylation Are Major Drivers of Gene Expression in K27M Mutant Pediatric High-Grade Gliomas. *Cancer Cell* **24**, 660–672 (2013).
34. Lewis, P. W. *et al.* Inhibition of PRC2 activity by a gain-of-function H3 mutation found in pediatric glioblastoma. *Science (1979)* **340**, 857–861 (2013).
35. Paugh, B. S. *et al.* Novel oncogenic PDGFRA mutations in pediatric high-grade gliomas. *Cancer Research* **73**, 6219–6229 (2013).
36. Roux, A. *et al.* High-grade gliomas in adolescents and young adults highlight histomolecular differences from their adult and pediatric counterparts. *Neuro-Oncology* **22**, 1190–1202 (2020).
37. D'Alessio, A., Proietti, G., Sica, G. & Scicchitano, B. M. Pathological and molecular features of glioblastoma and its peritumoral tissue. *Cancers (Basel)* **11**, (2019).
38. Jones, D. T. W. *et al.* Molecular characteristics and therapeutic vulnerabilities across paediatric solid tumours. *Nature Reviews Cancer* **19**, 420–438 (2019).
39. MacDonald, T. J., Aguilera, D. & Kramm, C. M. Treatment of high-grade glioma in children and adolescents. *Neuro-Oncology* **13**, 1049–1058 (2011).
40. Diwanji, T. P., Engelman, A., Snider, J. W. & Mohindra, P. Epidemiology, diagnosis, and optimal management of glioma in adolescents and young adults. *Adolescent Health, Medicine and Therapeutics Volume* **8**, 99–113 (2017).
41. Stupp, R. *et al.* Radiotherapy plus Concomitant and Adjuvant Temozolomide for Glioblastoma. *The New England Journal of Medicine* 987–996 (2005).
42. Warren, K. E. Diffuse intrinsic pontine glioma: poised for progress. *Frontiers in Oncology* **2**, (2012).
43. Piper, K., DePledge, L., Karsy, M. & Cobbs, C. Glioma Stem Cells as Immunotherapeutic Targets: Advancements and Challenges. *Frontiers in Oncology* **11**, (2021).
44. Aziz-Bose, R. & Monje, M. Diffuse intrinsic pontine glioma: Molecular landscape and emerging therapeutic targets. *Current Opinion in Oncology* **31**, 522–530 (2019).
45. Hashizume, R. *et al.* Pharmacologic inhibition of histone demethylation as a therapy for pediatric brainstem glioma. *Nature Medicine* **20**, 1394–1396 (2014).
46. Grasso, C. S. *et al.* Functionally defined therapeutic targets in diffuse intrinsic pontine glioma. *Nature Medicine* **21**, 555–559 (2015).
47. Liu, P. *et al.* Effects of oncolytic viruses and viral vectors on immunity in glioblastoma. *Gene Therapy* **29**, 115–126 (2022).

48. Varela-Guruceaga, M. *et al.* Oncolytic viruses as therapeutic tools for pediatric brain tumors. *Cancers (Basel)* **10**, (2018).
49. Jackson, H. J., Rafiq, S. & Brentjens, R. J. Driving CAR T-cells forward. *Nature Reviews Clinical Oncology* **13**, 370–383 (2016).
50. Zhang, C., Liu, J., Zhong, J. F. & Zhang, X. Engineering CAR-T cells. *Biomarker Research* **5**, (2017).
51. Mount, C. W. *et al.* Potent antitumor efficacy of anti-GD2 CAR T cells in H3-K27M+ diffuse midline gliomas letter. *Nature Medicine* **24**, 572–579 (2018).
52. Majzner, R. G. *et al.* GD2-CAR T cell therapy for H3K27M-mutated diffuse midline gliomas. *Nature* **603**, 934–941 (2022).
53. Lathia, J. D. *et al.* Distribution of CD133 reveals glioma stem cells self-renew through symmetric and asymmetric cell divisions. *Cell Death and Disease* **2**, (2011).
54. Singh, S. K. *et al.* Identification of a Cancer Stem Cell in Human Brain Tumors. *CANCER RESEARCH* **63**, 5821–5828 (2003).
55. Singh, S. K. *et al.* Identification of human brain tumour initiating cells. *Nature* **432**, 396–401 (2004).
56. Lathia, J. D., Mack, S. C., Mulkearns-Hubert, E. E., Valentim, C. L. L. & Rich, J. N. Cancer stem cells in glioblastoma. *Genes & Development* **29**, 1203–1217 (2015).
57. Lombard, A. *et al.* The Subventricular Zone, a Hideout for Adult and Pediatric High-Grade Glioma Stem Cells. *Frontiers in Oncology* vol. 10 (2021).
58. Adeberg, S. *et al.* Glioblastoma recurrence patterns after radiation therapy with regard to the subventricular zone. *International Journal of Radiation Oncology Biology Physics* **90**, 886–893 (2014).
59. Chaichana, K. L. *et al.* Relationship of glioblastoma multiforme to the lateral ventricles predicts survival following tumor resection. *Journal of Neuro-Oncology* **89**, 219–224 (2008).
60. Kroonen, J. *et al.* Human glioblastoma-initiating cells invade specifically the subventricular zones and olfactory bulbs of mice after striatal injection. *International Journal of Cancer* **129**, 574–585 (2011).
61. Goffart, N. *et al.* Adult mouse subventricular zones stimulate glioblastoma stem cells specific invasion through CXCL12/CXCR4 signaling. *Neuro-Oncology* **17**, 81–94 (2015).
62. Goffart, N. *et al.* CXCL12 mediates glioblastoma resistance to radiotherapy in the subventricular zone. *Neuro-Oncology* **19**, 66–77 (2017).
63. Mistry, A. M. *et al.* Association between supratentorial pediatric high-grade gliomas involved with the subventricular zone and decreased survival: A multi-institutional retrospective study. *Journal of Neurosurgery: Pediatrics* **26**, 288–294 (2020).

64. Qin, E. Y. *et al.* Neural Precursor-Derived Pleiotrophin Mediates Subventricular Zone Invasion by Glioma. *Cell* **170**, 845-859.e19 (2017).
65. Tomiyama, A., Kobayashi, T., Mori, K. & Ichimura, K. Protein phosphatases-a touchy enemy in the battle against glioblastomas: A review. *Cancers (Basel)* **11**, (2019).
66. Xu, Y. & Fisher, G. J. Receptor type protein tyrosine phosphatases (RPTPs) - Roles in signal transduction and human disease. *Journal of Cell Communication and Signaling* **6**, 125–138 (2012).
67. Kawachi, H. *et al.* Protein tyrosine phosphatase Z/RPTPb interacts with PSD-95/SAP90 family. *Molecular Brain Research* **72**, 47–54 (1999).
68. Fujikawa, A. *et al.* A head-to-toe dimerization has physiological relevance for ligand-induced inactivation of protein tyrosine receptor type Z. *Journal of Biological Chemistry* **294**, 14953–14965 (2019).
69. Xia, Z. *et al.* The expression, functions, interactions and prognostic values of PTPRZ1: A review and bioinformatic analysis. *J Cancer* **10**, 1663–1674 (2019).
70. Levy, J. B. *et al.* The Cloning of a Receptor-type Protein Tyrosine Phosphatase Expressed in the Central Nervous System. *THE JOURNAL OF BIOLOGICAL CHEMISTRY* **268**, 10573–10581 (1993).
71. Maurel, P., Rauch, U., Flad, M., Margolis, R. K. & Margolis, R. U. Phosphacan, a chondroitin sulfate proteoglycan of brain that interacts with neurons and neural cell-adhesion molecules, is an extracellular variant of a receptor-type protein tyrosine phosphatase. *Proceedings of the National Academy of Sciences* **91**, 2512–2516 (1994).
72. Navis, A. C. *et al.* Protein tyrosine phosphatases in glioma biology. *Acta Neuropathol* **119**, 157–175 (2010).
73. Lorente, G. *et al.* Functional comparison of long and short splice forms of RPTP $\beta$ : Implications for glioblastoma treatment. *Neuro-Oncology* **7**, 154–163 (2005).
74. Chow, J. P. H., Fujikawa, A., Shimizu, H., Suzuki, R. & Noda, M. Metalloproteinase- and  $\gamma$ -secretase-mediated cleavage of protein-tyrosine phosphatase receptor type Z. *Journal of Biological Chemistry* **283**, 30879–30889 (2008).
75. Papadimitriou, E. *et al.* Pleiotrophin and its receptor protein tyrosine phosphatase beta/zeta as regulators of angiogenesis and cancer. *Biochimica et Biophysica Acta - Reviews on Cancer* **1866**, 252–265 (2016).
76. Müller, S. *et al.* A role for receptor tyrosine phosphatase $\zeta$  in glioma cell migration. *Oncogene* **22**, 6661–6668 (2003).
77. Fujikawa, A. & Noda, M. Role of pleiotrophin-protein tyrosine phosphatase receptor type Z signaling in myelination. *NEURAL REGENERATION RESEARCH* **11**, 549–551 (2016).
78. Fujikawa, A. *et al.* Consensus substrate sequence for protein-tyrosine phosphatase receptor type Z. *Journal of Biological Chemistry* **286**, 37137–37146 (2011).

79. Kuboyama, K., Fujikawa, A., Suzuki, R., Tanga, N. & Noda, M. Role of chondroitin sulfate (CS) modification in the regulation of protein-tyrosine phosphatase receptor type Z (PTPRZ) activity: Pleiotrophin-PTPRZ-A signaling is involved in oligodendrocyte differentiation. *Journal of Biological Chemistry* **291**, 18117–18128 (2016).
80. Asai, H., Yokoyama, S., Morita, S., Maeda, N. & Miyata, S. Functional difference of receptor-type protein tyrosine phosphatase  $\zeta/\beta$  isoforms in neurogenesis of hippocampal neurons. *Neuroscience* **164**, 1020–1030 (2009).
81. Ulbricht, U. *et al.* Expression and Function of the Receptor Protein Tyrosine Phosphatase and Its Ligand Pleiotrophin in Human Astrocytomas. *Journal of Neuropathology and Experimental Neurology* **62**, 1265–1275 (2003).
82. Bourgonje, A. M. *et al.* Intracellular and extracellular domains of protein tyrosine phosphatase PTPRZ-B differentially regulate glioma cell growth and motility. *Oncotarget* **5**, 8690–8702 (2014).
83. Koutsioumpa, M. *et al.* Receptor protein tyrosine phosphatase beta/zeta is a functional binding partner for vascular endothelial growth factor. *Molecular Cancer* **14**, (2015).
84. Fujikawa, A. *et al.* Targeting PTPRZ inhibits stem cell-like properties and tumorigenicity in glioblastoma cells. *Scientific Reports* **7**, (2017).
85. Fujikawa, A. *et al.* Small-molecule inhibition of PTPRZ reduces tumor growth in a rat model of glioblastoma. *Scientific Reports* **6**, (2016).
86. Yamanoi, Y. *et al.* Soluble protein tyrosine phosphatase receptor type Z (PTPRZ) in cerebrospinal fluid is a potential diagnostic marker for glioma. *Neuro-Oncology Advances* **2**, 1–12 (2020).
87. Knudsen, A. M. *et al.* Surgical resection of glioblastomas induces pleiotrophin-mediated self-renewal of glioblastoma stem cells in recurrent tumors. *Neuro-Oncology* (2021).
88. Huang, P. *et al.* Chemotherapy-driven increases in the CDKN1A/PTN/PTPRZ1 axis promote chemoresistance by activating the NF- $\kappa$ B pathway in breast cancer cells. *Cell Communication and Signaling* **16**, 1–12 (2018).
89. Shi, Y. *et al.* Tumour-associated macrophages secrete pleiotrophin to promote PTPRZ1 signalling in glioblastoma stem cells for tumour growth. *Nature Communications* **8**, (2017).
90. Deuel, T. F. Anaplastic lymphoma kinase: “Ligand Independent Activation” mediated by the PTN/RPTP $\beta/\zeta$  signaling pathway. *Biochimica et Biophysica Acta - Proteins and Proteomics* **1834**, 2219–2223 (2013).
91. Wang, X. Pleiotrophin: Activity and mechanism. in *Advances in Clinical Chemistry* vol. 98 51–89 (Academic Press Inc., 2020).